Validation of 3D Motion Capture Protocols aimed at the Analysis of Human Gait and Run

Paula Flórez Herrera

Table of Contents

Validation of 3D Motion Capture Protocols aimed at the Analysis of Human Gait and Run

1. INTRODUCTION

Gait analysis is a field of research where the standardization of data between investigation centers is crucial for the validity of the conclusions that could be drawn from these results. There are several methods for the characterization and analysis of human gait, commonly known as protocols (Ferrari, et al., 2008).

It is common for research centers to use a protocol that has already been published due to the validity of its results instead of developing a new design, this also eases the direct comparison of resulting data to another dataset already collected with said protocol. However, many research centers choose to modify existing protocols for a variety of reasons, in order to adapt them to their motion capture system, environment, testing subject, among others (Ferrari, et al., 2008). STT Systems did this, basing their main gait analysis software (Clinical 3DMA) on the well-known Helen Hayes protocol, but slightly altering it in order to obtain more information during the trials.

Upon carefully examining the original literature that defines the Helen Hayes protocol (Kadaba, Ramakrishnan, & Wootten, 1990) in contrast with the current code behind the Clinical 3DMA System in STT, a detailed divergence report was compiled, analyzing the theoretical differences found between both protocols. The same was done for the EDDO/ACE Protocol, which also derives from the original Helen Hayes but it was modified for visibility of a portable motion capture system as well as adapted to running gait.

Mainly, the current study will identify the sources of the divergences between the abovementioned protocols in order to correct possible discrepancies or document notable result changes for the validation of the EDDO/ACE Running protocol based on the STT adapted Helen Hayes protocol.

2. OBJECTIVES

- Understand the architecture of the gait analysis protocols used by the system and cited from the literature.
- Compare the current STT Systems protocol with the original Helen Hayes literature and analyze the possible repercussions of the differences between them in the final results of the gait analysis.
- Evaluate the possibility of using the same protocol for gait and run analysis.
- Perform a full validation of the protocol Lower-Body Configuration for Portable 3D Gait Analysis EDDO/ACE Running from STT modified from the Helen Hayes Protocol.
- Analyze the results from field data collection using the EDDO/ACE protocol and the STT Helen Hayes adaptation as a base for comparison.
- Understand the effect of the different parameters on the final curves.

3. MOTION CAPTURE AND GAIT ANALYISIS BASICS

3.1. Terminology

Some of the most used terms in the study are presented in this section, the definitions were collected from the STT documentation throughout the project development:

Anatomy of the human body:

Pelvis: Comprises the pelvic bone and the lumbar area of the human body, between the abdomen and the thighs.

Thigh: Comprises the femur and its surrounding tissue, extending from the hip joint to the knee joint.

Shank or calf: Comprises the tibia and fibula and their surrounding tissues, extending from the knee joint to the ankle joint.

Foot: For the purpose of biomechanical studies, the foot is defined as a rigid segment extending from the calcaneus bone to the tip of the toes, below the ankle joint.

Coronal plane: One of the main body planes. Divides the body in an anterior half (front) and a posterior half (back). Perpendicular to both sagittal and transverse planes.

Sagittal plane: One of the main body planes. Divides the body in a right half and a left half. Perpendicular to both coronal and transverse planes.

Transverse or horizontal plane: One of the main body planes. Divides the body in a cranial half (upper) and a caudal half (lower). Perpendicular to both coronal and sagittal planes.

Anatomical reference position: Refers to the position of the human body considered "resting" and used as a reference to locate points using directions relative to body landmarks. The subject is considered standing with their feet at shoulder width, facing front with their toes pointing at the same direction, spine straight, arms resting at each side with palms facing forward (thumbs pointing out), and looking straight ahead.

Motion capture:

Marker: There are several types of markers in biomechanics, for the purpose of clarity, all markers used and mentioned in this project are reflective markers of 1 centimeter diameter attached to either a plastic base or a plastic extensor unless it is stated otherwise.

Motion capture system: Motion capture system refers to the hardware setup used to record the subject during a gait analysis test: cameras, force and pressure plates, inertial sensors, electromyography sensors and computer, in general.

Gait analysis:

Gait analysis protocol: A protocol refers to a series of parameters that are followed to obtain the final results of the gait analysis, these include the marker set placement on the subject (quantity and types of markers and their specific locations) and the measurements performed before or after the tests.

Biomechanical model: A biomechanical model refers to the geometrical, anatomical, and physical calculations performed to obtain the final results of a gait analysis given the data obtained from a motion capture system using a specific protocol. In this way, several protocols can share a biomechanical model or parts of it, and be acquired with different motion capture systems.

Gait cycle: Refers to the parameterized set of events that define the way a subject walks. A normal gait cycle starts with the heel strike of the foot on the side being analyzed (typically 0% of the gait cycle) and ends with the following heel strike of the same foot (100% of the same gait cycle). The entirety of a subject walking can be divided in gait cycles that will be different depending on the side being observed.

Stance phase: Part of the gait cycle when the foot is in contact with the ground.

Toe off: Part of the gait cycle when the toes of the foot separate from the ground.

Swing phase: Part of the gait cycle when the foot is not in contact with the ground and the leg swings in the air.

Heel strike: Part of the gait cycle when the heel of the foot makes first contact with the ground after the swing phase during walking.

Step: A step is defined as the period between the heel strike of one foot and the subsequent heel strike of the opposite foot.

Stride: A stride is defined as the period between the heel strike of one foot and the subsequent heel strike of the same foot, or two complementary steps.

Trial: A trial is defined as an entire capture done with the motion capture system while the subject walks within the capture area.

3.2. Motion Capture – State of the Art

Motion capture technology is used to record movement for a great variety of uses, from animation of movies and videogames to the clinical analysis of the human body. Depending on the different requirements and purposes, several forms of motion capture systems can be found in the literature (Imagine Media, 1995).

An example of a type of motion capture system is inertial sensors, which use accelerometers and gyroscopes to calculate the position, orientation and speed of each segment of the body and send the collected data wirelessly to a computer. The data is then processed in order to track the movement of the joints (Roetenberg, Luinge, & Slycke, 2013).

There are, however, other types of motion capture systems that use cameras to record motion in a delimited space, optical systems (Sigal, 2012). The particular type of optical system used for this study was an optical system with passive markers. It uses optoelectronic cameras that emit light that is then reflected by markers coated with retro-reflective materials, and the camera lenses record the bright reflections of the markers that are inside the capture area of the camera. Multiple cameras aimed at the same capture volume from different angles can generate enough data to triangulate the 3D position of the markers in space relative to an origin point (Imagine Media, 1995).

Currently, STT has a passive marker optical system with 6 cameras installed in a 10x7m testing room and a portable passive marker optical system with 3 cameras in a solid bar that attaches to a tripod for easy transportation. Both of these systems were used for the study in the designated capture area at STT.

3.3. Gait Analysis – Architecture of Human Gait and Run Protocols

In order to analyze the way the human body moves, motion capture systems use different strategies to place the markers that will provide the kinematic information for the analysis. A protocol consists of a predetermined specification of the quantity and location of markers placed on the body as well as a biomechanical model that determines the calculations needed to obtain results from the raw position/time data obtained from the markers with the motion capture system (Ferrari, et al., 2008).

There are several protocols reported in the literature, all with different purposes, advantages and limitations. However, some protocols are common in the field of lower limb analysis of gait such as the Helen Hayes protocol, originally known as the 'Newington model'. This protocol is considered the pioneer technique for data acquisition and has been used and modified since it first made an appearance in the literature in the late 1980's (Ferrari, et al., 2008).

The Newington model has been modified over the years and some of its most used applications are the Plug-In Gait model used by Vicon Motion Systems (PiG – Vicon Motion Systems, Oxford, UK) and the Davis model used by BTS Bioengineering (SMART-DX – BTS Bioengineering, MI, Italy) for their commercial software products aimed at clinical gait and motion analysis.

Other examples of common protocols are the LAMB protocol, developed by an Italian gait analysis laboratory (Laboratorio per l'Analisi del Movimento nel Bambino) which uses 19 markers for lower train analysis, the Total 3D Gait developed by the Rizzoli Gait Orthopedic Institute which uses 20 markers and the slightly differently oriented CAST protocol (Calibration Anatomical System Technique) which differentiates internal from external anatomical landmarks with 22 markers in total (Ferrari, et al., 2008).

STT uses a common adaptation of the Helen Hayes protocol (which will be further explained in the following sections) and uses it as their default acquisition protocol for gait analysis. STT has developed new protocols aimed at the analysis of gait and run that require a thorough validation, which will be done using the Helen Hayes adapted protocol as the gold standard.

3.4. Clinical Gait Analysis – The Helen Hayes Protocol

The Helen Hayes Protocol (HH) gets its name from the Helen Hayes Hospital in New York, USA, where it was first used as a formal Lower Train Gait Analysis Protocol. The protocol was based off of a hip joint rotation center calculation developed in the Newington Children's Hospital in Connecticut, USA (the original 'Newington model'), which was developed through the radiographic examination of 25 patients (Davis, Ounpuu, Tyburski, & Gage, 1991). The Helen Hayes Protocol was published in the paper "Measurement of lower extremity kinematics during level walking", and has since become one of the most commonly used and adapted gait analysis protocols in the field (Kadaba, Ramakrishnan, & Wootten, 1990).

The protocol uses 15 reflective markers (placed on the sacrum, both Anterior Superior Iliac Spines, both great trochanters, both thighs, both femoral epicondyles, both shanks, both lateral malleoli and both 2^{nd}-3^{rd} toe junctures) and uses their locations to determine hip, knee and ankle joint centers, which in turn define the angles for these joints throughout a gait cycle (defined as heel strike to immediately following heel strike) in all three of the main body planes.

The following section encompasses a comparison between the original Helen Hayes protocol and the STT adapted version of the Helen Hayes protocol that will be used for the validation of the STT-designed EDDO/ACE protocol (EDDO Running).

4. CLINICAL 3DMA HELEN HAYES PROTOCOL (STT SYSTEMS)

4.1. Divergence Report (STT HH – HH)

The first step for the validation of the STT Adapted Helen Hayes Protocol (STT HH) was a thorough revision of the original literature and the source code for the biomechanics of the STT software, in order to understand the way the angles are calculated on each of them, how both methods differ and the influence these differences might have on the final result of the gait analysis. A complete review of the different aspects of both protocols is presented in the following sections.

4.1.1.Marker System

The marker system of a protocol defines the input information that the biomechanical model of gait is going to obtain from the capture. Each marker placed on the subject yields a location (X, Y and Z) in the capture area for each frame of the trial. It is important that the marker positions are (1) identifiable on the subject, for example bone protrusions that are either palpable or visible on the skin, and (2) located in a point that yields useful information for the model, such as near the center of rotation of a joint or a segment of a bone that retains a measurable relation to the location of said center of rotation.

Both the original HH and STT HH protocol use 15 reflective markers, 4 of which are attached to extensor bars in order to increase their visibility from the cameras. In both cases, the 15 markers are distributed between the subject's pelvic bone, femurs, tibias and feet as it is shown both in ***Table 1*** and ***Figure 1***.

Table 1. Marker system comparison

Marker		Original HH	STT HH
PELVIS	**Sacrum** at L5	Yes	Yes
	Anterior Superior Iliac Spines (ASIS) Left and Right	Yes	Yes
FEMUR	**Greater Trochanters** Left and Right (femoral epiphysis)	Yes	No
	Thighs Left and Right (approximately in the middle of the thigh with an extensor bar)	Yes	Yes
	Knees Left and Right (lateral femoral epicondyle)	Yes	Yes
TIBIA	**Shanks** Left and Right (approximately in the middle of the shank with an extensor bar)	Yes	Yes
	Ankles Left and Right (lateral malleolus)	Yes	Yes
FOOT	**Heels** Left and Right (calcaneus)	No	Yes
	Toes Left and Right (second phalange between the second and third toe)	Yes	Yes
Total Markers		**15**	**15**

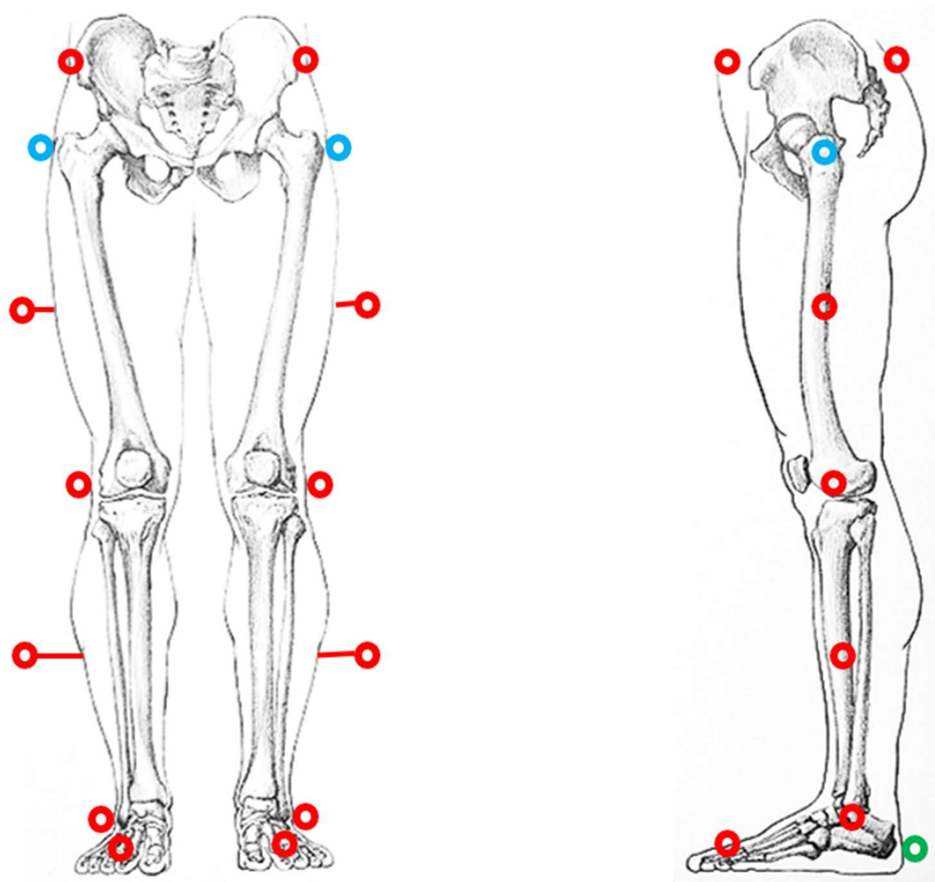

Figure 1. Helen Hayes marker systems: Original (red and blue) and STT HH (red and green). Original image reference *(Drawing Academy, 2015)*

As ***Figure 1*** shows, the key difference between these two protocols is that the STT HH dismisses the markers located at the great trochanters (blue circles in Figure 1) and replaces them with markers on both heels (green circles in ***Figure 1***). The removal of the great trochanter markers has no effect in the biomechanical calculations of the model, since the center of rotation for the hip joint is a function of the ASIS markers locations and the standard angles of the pelvic bone, which were measured by the Newington Children's Hospital for their hip center calculation method through the radiographic examination of 25 patients (Davis, Ounpuu, Tyburski, & Gage, 1991).

The biomechanical model used by STT calculates the pelvic geometry the same way it is done in the original literature using the ASIS and sacrum markers, and it proceeds by computing the hip, knee and ankle joint centers as well as the thigh and shank geometry using the information from the original HH markers (Kadaba, Ramakrishnan, & Wootten, 1990).

As for the added heel markers in the STT HH marker system, they provide enough information to expand the original biomechanical model to include not only pelvis, thigh and shank geometry but also foot geometry, which results in the calculation of ankle inversion-eversion and foot rotation angles additional to the angles that could already be obtained from the original HH model (all of which are further explained in ***Table 2*** in the following section).

4.1.2.Coordinate Systems

The basis of a biomechanical model computation for gait analysis is the description of rotations in space using a modification of the Euler angles. The Euler angles represent the orientation of a solid object in relation to a reference coordinate system, in the case of biomechanics, three elemental rotations for a tridimensional space (Smith, 2000). These angles are measured using predefined coordinate sets as a reference for the different body segments, the definition and distribution of which will be explained in the following segments.

The original HH model and the STT HH version have a slightly different approach when setting the reference coordinates for the angle calculations. ***Figure 2*** shows a schematic of the reference coordinate sets used for each body segment as well as the global coordinates of the whole body model. These reference systems are obtained by computing the location data from the capture of the reflective markers on the subject as they move, using the known points of the subject's anatomy to estimate as truthfully as possible the locations of centers of mass and rotation of the rest of the body segments.

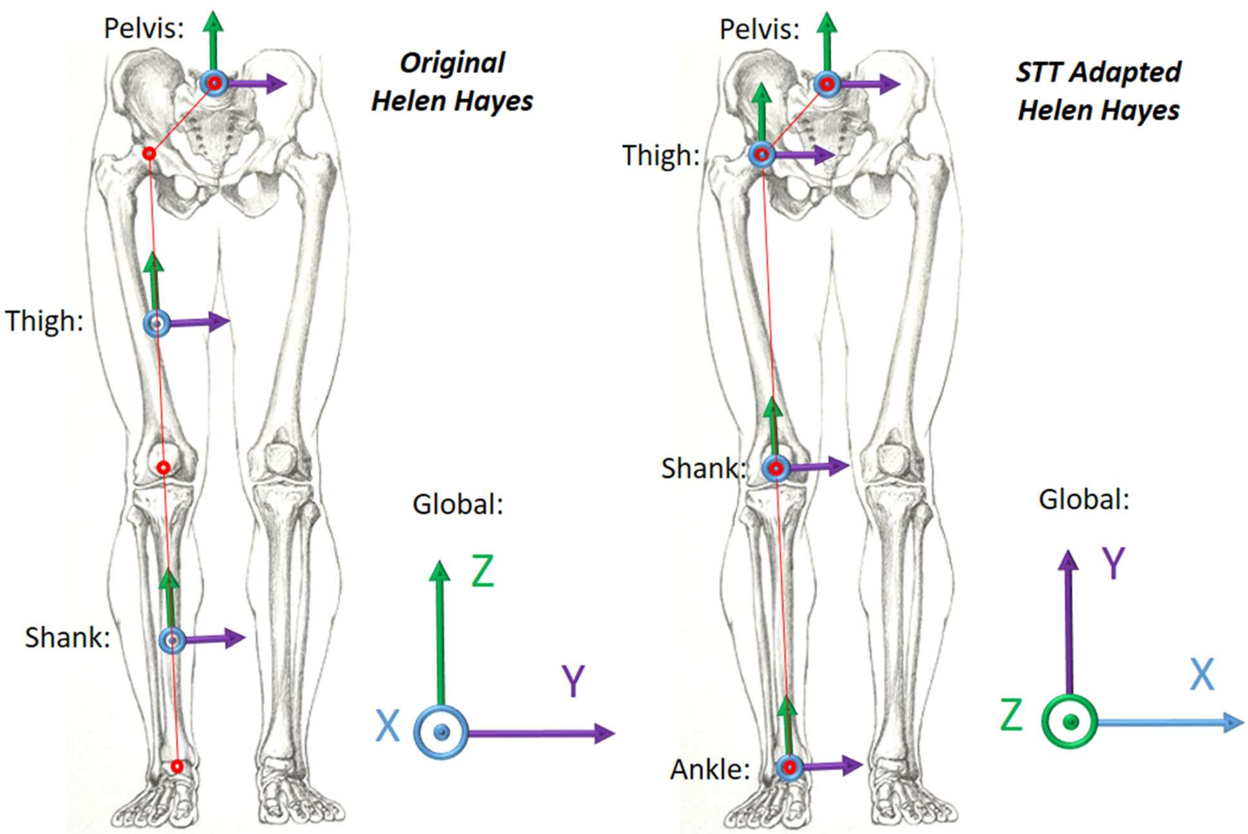

Figure 2. Coordinate systems for Helen Hayes: Original (left) and STT modified version (right). The red circles represent the anatomical centers of rotation of each joint and the axes represent the coordinate system associated with them and their orientation.

The original HH locates its reference systems for the thigh and shank in the middle point of the respective body segment along the lines connecting the anatomical centers of rotation of the joints. Meanwhile, the STT HH protocol displaces the reference axes to the respective center of rotation itself, and also includes an extra reference axis for the ankle and foot segment.

Figure 2 also shows that while the local reference axes in the original model are oriented the same way as the local reference axes in the STT HH model, the global reference coordinate sets are not equal. The global sets in each model are used to orient the subject within the capture space. In the original HH, the global axes are oriented in the same way as the local axes, presumably to facilitate the nomenclature, while in the STT HH model it is different. The effect of this difference, however, is inexistent, since the angles are always measured by comparing the appropriate axis equivalent (the pelvic Z is compared to its true global equivalent, the global Y, instead of its apparent equivalent, the global Z, and so on).

In the STT HH model, the displacement of the reference axes is taken into account when computing the angles, and the resulting angles are equivalent to those calculated in the original HH protocol. The complete set of angles computed by the STT HH model and that will be used to compare the outcomes of the trials are described in ***Table 2***.

Table 2. Measured Joint Angles

	Along the local Y angle	**Along the local X angle**	**Along the local Z angle**
Pelvis	Pelvic Tilt *(Anterior/Posterior)*	Pelvic Obliquity *(Superior/Inferior)*	Pelvic Rotation *(External/Internal)*
Hip	Hip Flexion *(Flexion/Extension)*	Hip Add-Abduction *(Adduction/Abduction)*	Hip Rotation *(External/Internal)*
Knee	Knee Flexion *(Flexion/Extension)*	Knee Varus-Valgus *(Varus/Valgus)*	Knee Rotation *(External/Internal)*
Ankle	Ankle Flexion *(Plantar/Dorsal flexion)*	Ankle Inv-Eversion *(Inversion/Eversion or Supination/Pronation)*	Ankle Rotation *(External/Internal)*
Foot	~	~	Foot Rotation *(External/Internal)*

A total of 5 joints are evaluated in the STT HH model, the first 4 each yield an angle for each of the main 3 body planes (coronal or literature's global X, sagittal or literature's global Y and transverse or literature's global Z), the last joint only provides an angle for the transverse plane.

4.1.3. Euler Angles Sequence

One of the defining characteristics of Euler angles is that the final orientation of the solid object depends not only on the individual rotation of the Euler angles but also on the order in which these motions are performed (Smith, 2000). The angle order in the original Helen Hayes literature and in the STT HH version are different, as it is shown in ***Table 3***, but it has to be taken into account that for the calculation of orientations of free-moving bodies in space, the effect of altering the order of the Euler angles is much greater than in limited-movement systems such as the human legs.

Both protocols start by computing the Y axis rotation (in the global sagittal plane), mainly because this rotation is the most significant one during the typical motions required for human locomotion. After this, the literature reports calculating the X axis rotation (in the global coronal plane) followed by the Z axis rotation (in the global transverse plane) while the STT protocol computes the Z axis rotation followed by the X axis rotation, instead.

Table 3. Euler angles comparison for all joints

Angle	Original Helen Hayes	STT Helen Hayes
1st	Y axis *Tilt, Flexion-Extension*	Y axis *Tilt, Flexion-Extension*
2nd	X axis *List, Obliquity, Add-Abduction, Inv-Eversion*	Z axis *Rotation*
3rd	Z axis *Rotation*	X axis *List, Obliquity, Add-Abduction, Inv-Eversion*

The STT approach to the rotation sequence modifies the original protocol in order to reduce error in the measurements, this is done by computing the most significant rotation first, then the second most significant and leaving the least significant to be computed last (YZX or Flexion-Rotation-Obliquity). Even though trials have not been conducted to verify the error reduction when altering the order of the last two Euler angles, the results of gait analysis tests done with the STT HH protocol highly resemble the normative datasets found in the literature using the Helen Hayes original protocol (Le Borgne & Bontempi, 2013), which suggests that the effect of the modification of the Euler sequence in a limited-movement system does not modify the outcome enough to be noticeable for the purposes of gait analysis.

4.1.4.Angle Nomenclature

Lastly, it was important to take note of the differences in the nomenclature used for the resulting measured angles in order to identify possible errors when comparing gait data between both protocols. ***Table 4*** shows the direction considered as positive (+) when measuring each of the angles of ***Table 2*** for both protocols.

Table 4. Angle Nomenclature

Joint	Angle	Positive Direction in Original HH	Positive Direction in STT HH
PELVIS	Tilt	Posterior	Anterior
	Obliquity	Differs for right & left	Superior
	Rotation	Differs for right & left	Internal
HIP	Flexion	Extension	Flexion
	Add-Abduction	Differs for right & left	Adduction
	Rotation	Differs for right & left	Internal
KNEE	Flexion	Flexion	Flexion
	Varus-Valgus	Differs for right & left	Valgus
	Rotation	Differs for right & left	Internal
ANKLE	Flexion	Plantar Flexion	Dorsal Flexion
	Inv-Eversion	Differs for right & left	Inversion
	Rotation	Differs for right & left	Internal
FOOT	Rotation	Not Calculated	Internal

In order to provide visual representation of the angle directions mentioned in ***Table 4***, a diagram of all the rotation names is presented in ***Figure 3***. Also, the reference positions in which each of the measured angles is 0° were also examined and both protocols assume 0° rotation for all their angles when the body segments are in anatomical reference position as presented in ***Figure 3***.

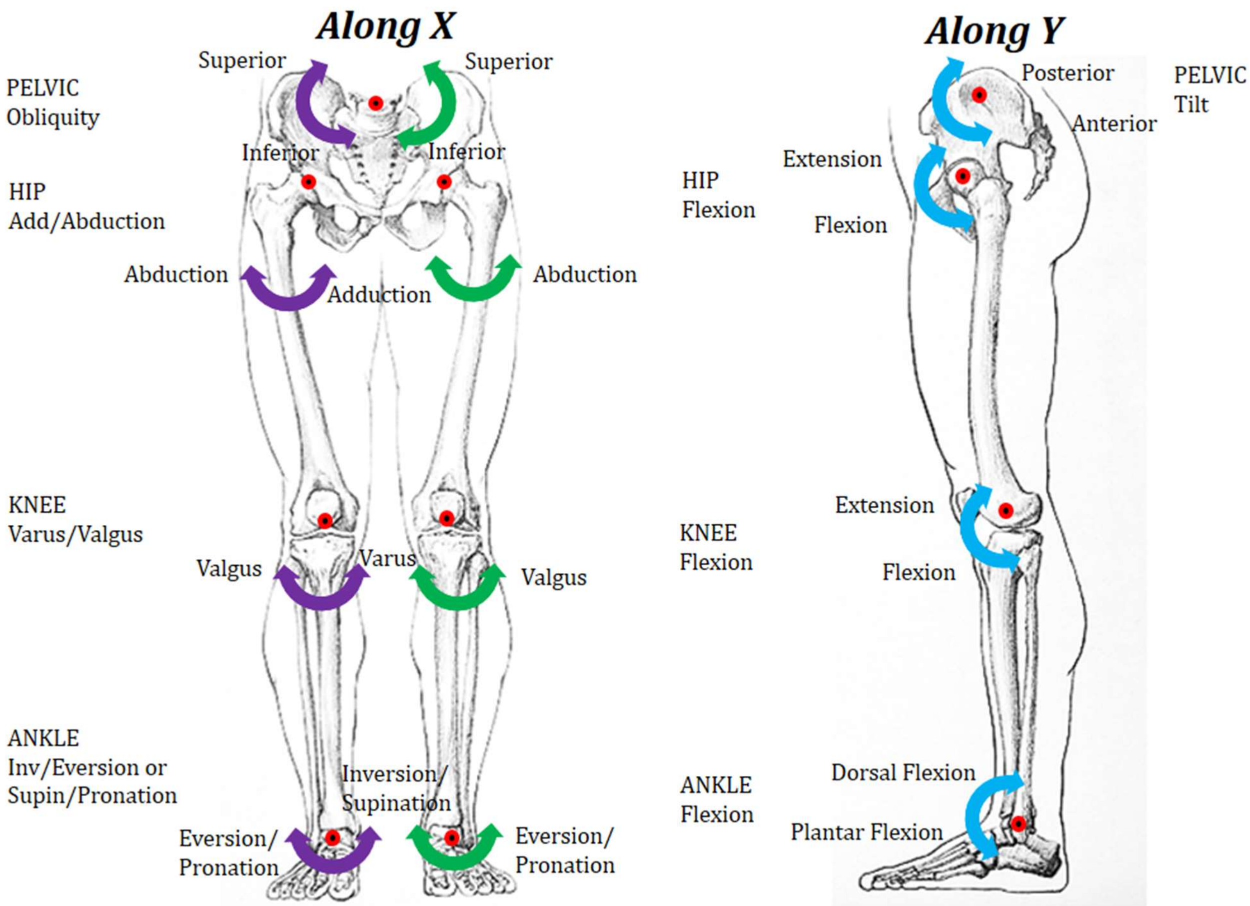

Figure 3. Reference of Angle Nomenclature. Left: coronal plane view. Right: sagittal plane view.

As it is summarized in ***Table 4***, the STT HH protocol modified several of the positive angle directions used in the original literature. This was done in order to simplify the understanding of the final graphs by having each angle represent similar or somewhat equivalent rotations on each of the evaluated joints (having all internal rotations be positive for right joints as well as for left joints, or hip and knee flexion both being positive).

It is the case for angles such as the rotations along the X axis that the assignment of a positive direction was done according to the available literature, from which the normal curves were extracted to compare with the obtained gait data.

The modifications to the nomenclature explained above do not alter the final results of the biomechanical model, since the values remain the same and only the visualization of the data is changed in order to simplify its comparison with trials done by either the STT system or any other gait analysis protocol or software.

4.2. Current Normative Database

A normative database is a set of data that comprises the averaged data of the angles of different joints throughout the gait cycle for several test subjects, in order to have a way of comparing the results of a gait analysis trial. Normative databases aim to describe the typical curves of movement during gait for different groups of people (by age, gender, different motor pathologies, speed, ethnicity, and more). Most common normative databases include normal speed walking for adults and children of different countries, and they are used as a basis of comparison in clinical reports of gait analysis. The data is normally presented against the gait cycle represented in percentage, where 0% is the initial contact of the respective side foot on the ground and 100% is the immediate next initial contact of the same side foot on the ground (with the toe-off of the respective foot normally around 60%).

In the case of STT Systems, the gait analysis software produces a report with graphs that compare the trial result to a normal curve of the same joint and angle taken from an American normative database (Le Borgne & Bontempi, 2013). Some of the normal curves obtained from the database are shown on ***Figure 4*** in gray, which is the way they are usually presented in the gait analysis reports. The other curves are from a random test trial and they are also represented as they usually are for the STT software reports.

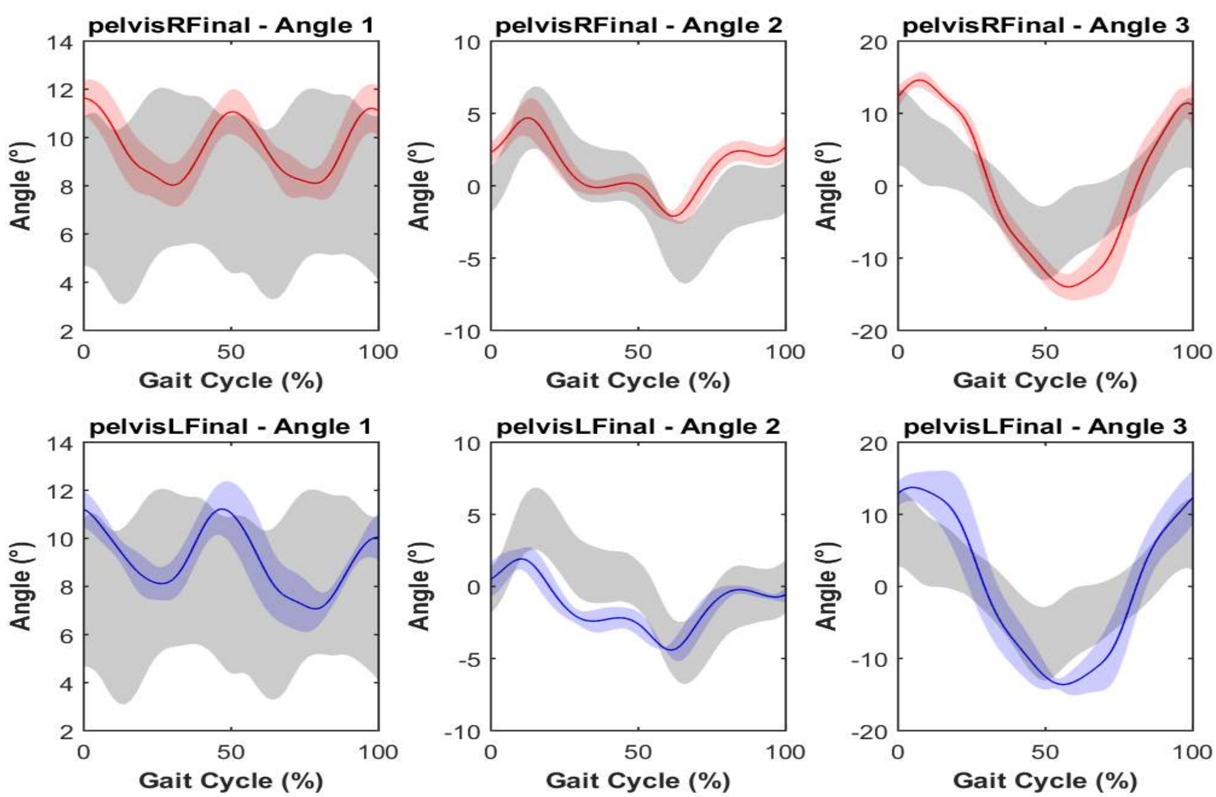

Figure 4. Example of the normative curves (gray) with a random walking trial (red for the right side, blue for the left side) for all the angles (Tilt in Angle 1, Obliquity in Angle 2 and Rotation in Angle 3) of the pelvic joint, mean values in a solid line and standard deviation as a colored area.

Since the normative database that is currently being used for the reports is not very recent and based in another continent, it was determined that it would be ideal to compare it to more recent databases located as close to the local population as possible in order to confirm its validity.

Two databases were selected for the comparison with the current normative after a literature review that aimed for normal walking curves of as many patients as possible (Gillette Children's in the United States) (Schwartz, Rozumalski, & Trost, 2008) and studies based in Europe (Fondazione Don C. Gnocchi in Italy) (Bovi, Rabuffetti, Mazzoleni, & Ferrarin, 2011).

Both new normatives and the current STT Systems normative were compared and a few differences were found, an example of which is shown on the ankle flexion data in ***Figure 5***. The data shows differences that could significantly alter the clinical evaluation of patient data.

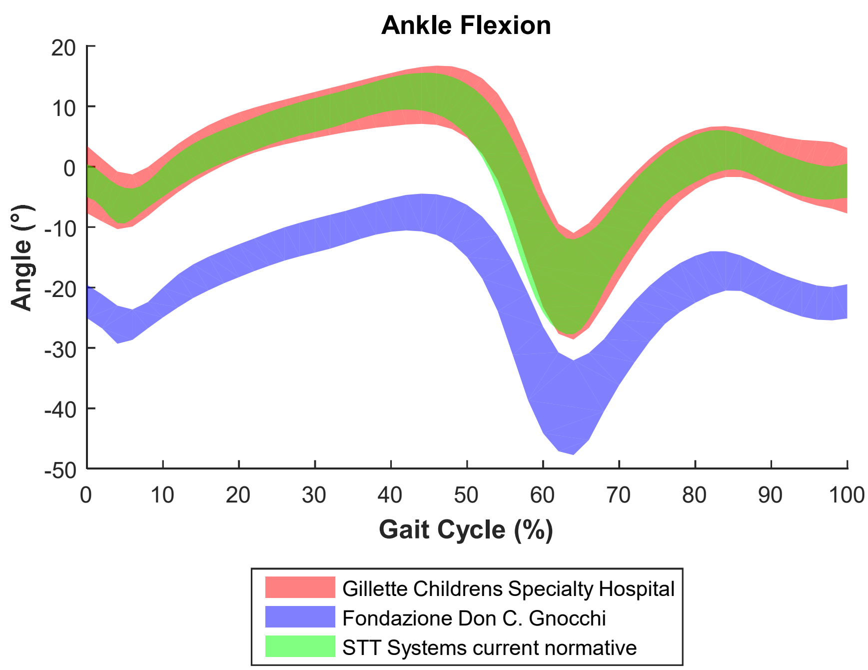

Figure 5. Normative database comparison for ankle flexion

The Italian database (Fondazione Don C. Gnocchi) shows a significant offset when compared to both American databases. This could be a direct result from the gait analysis protocols used for the examination (Gillette used a functional protocol, Don C. Gnocchi used the LAMB protocol and the current STT Systems reference normative used a modified Helen Hayes protocol (Le Borgne & Bontempi, 2013)) or an offset definition issue.

Since the documentation of the normatives does not provide enough information to conclusively decide where the discrepancy might come from, it was recommended that the data obtained from the non-pathological patients tested for the protocol validation within this project, is used to create a new local STT Systems normative database for gait analysis, and that this is the gait normative used for the generation of reports in the STT software. This new database could much more significantly resemble the gait patterns of patients and subjects from the south of Europe than an American database.

4.3. Running Analysis: Difficulties and limitations

Aside from walking, running is another form of locomotion that could be analyzed using motion capture systems and gait protocols. The analysis of running, however, has proven to be slightly more complicated than that of walking, due to a few variations that occur between the two forms of locomotion.

One of the key problems of running analysis towards the beginning of motion capture systems was the vibration. During running, the force of the foot strike and the speed of the swing phase generate a great amount of noise in the marker capture, which used to cause a fundamental problem when trying to track the markers for the biomechanical model computations. Currently, filtering methods and high frequency cameras facilitate the reduction of vibration induced noise in trials, not fully but enough to be able to analyze the results of the trials without being significantly influenced by noise.

Another crucial difference between the analysis of gait and run is the knee singularity problem. During running, knee flexion surpasses 90°, which is a singular position for this joint (as it happens with other joints in the body such as the shoulder and the wrist). In order to properly analyze running gait, new protocols had to be developed to overcome the obstacles that would present themselves if a normal gait protocol was used.

STT Systems designed their own running analysis protocol named EDDO/ACE Running, based on the same Helen Hayes protocol described in this previous section, with some important differences in order to accommodate it not only for running analysis but also for a portable motion capture system acquisition, which would facilitate the transport and setup of a motion analysis laboratory.

In the following section, the entire EDDO/ACE Running protocol is presented and compared to the STT Helen Hayes Protocol in order to determine the sources of the potential differences between both protocols and analyze the validity of the EDDO protocol for walking and running analysis when compared to a protocol that is already proven to be not significantly different from the literature references for gait analysis.

5. EDDO RUNNING PROTOCOL (STT SYSTEMS)

The EDDO/ACE protocol or EDDO Running protocol proposes a modification to the STT HH protocol in order to use a portable motion capture system and also expand the application of the biomechanical model by adapting it to running analysis.

In order to use the portable motion capture system previously mentioned, which consists of three cameras on a horizontal bar attached to a tripod, the EDDO protocol adapts its marker system to ensure a balance between visibility and amount of information. This modification requires a different biomechanical model calculation, but aims to result in the same angles measured in the original Helen Hayes protocol, which is what will be discussed in the observed results.

As for the expansion into running analysis, several modifications had to be put in place in the biomechanical model in order to account for the crucial differences between gait and run, and these will be explained further in the upcoming sections.

5.1. Marker System

The EDDO Protocol required all its markers to be visible when using the portable motion capture system previously described, which resulted in additions and modifications of the adapted STT Helen Hayes protocol. For one, the EDDO setup would have the three-camera system record the subject from the back, so front facing markers were relocated (Anterior Superior Iliac Spines to Posterior Superior Iliac Spines, and Toes to Lateral Feet). A few extra markers were also added in order to complement the resulting marker system (an extra marker at L1 in the Lumbar region and two extra markers for the Great Trochanter of each femoral head). The final marker set for the EDDO Running Protocol is fully described in ***Table 5*** and a diagram of the final ideal positions of the markers is presented on ***Figure 6***.

Table 5. Marker system for the EDDO (ACE) Protocol

Segment	Marker
PELVIS	**Lumbar** at L1
	Posterior Superior Iliac Spines (PSIS) Left and Right
	Sacrum at L5
FEMUR	**Greater Trochanters** Left and Right (femoral epiphysis)
	Thighs Left and Right (approximately in the middle of the thigh with an extensor bar)
	Knees Left and Right (lateral femoral epicondyle with a small extensor bar)
TIBIA	**Shanks** Left and Right (approximately in the middle of the shank with an extensor bar)
	Ankles Left and Right (lateral malleolus)
FOOT	**Heels** Left and Right (calcaneus)
	Lateral Heels Left and Right (vertically aligned with the Ankle marker and levelled with the Heel marker, forming a 90° angle between them)
Total Markers	**18**

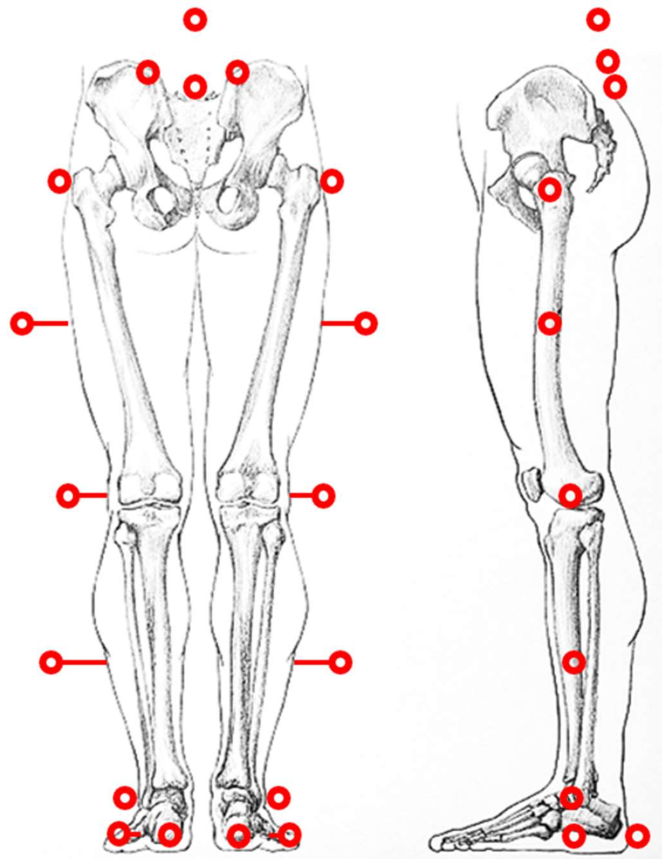

Figure 6. Marker System for the EDDO Protocol. Left: Back view. Right: Lateral view.

As shown on ***Figure 6***, the thigh and shank markers remain attached to extensor bars as they were for the Helen Hayes protocol, in addition, the EDDO protocol places the knee and lateral heel markers on smaller extensor bars in order to increase their visibility with the new capture system.

5.2. Calibration Position

In order to ensure the best quality of the analysis, the EDDO protocol requires a calibration of the marker system before the trials. This is done by capturing a few seconds of the subject standing still with all markers on, in order to register the distances between the markers at anatomical position and use them as a reference point for further movements within the trial.

The system allows to capture data without a calibration, however, the results after testing both options show a better adjustment of the protocol for the trials with a previous calibration due to the possibility to compare the relative marker positions for the different stages of gait in a protocol with limited input data regarding the capture system setup.

5.3. Calculation of Joint Centers of Rotation

The EDDO protocol attempts to use the information of its marker system to recreate a biomechanical model that can measure the same joint angles as the Helen Hayes protocols. The main order of the calculation remains, starting from the pelvic joint and ending with the feet.

Without the ASIS markers, the PSIS and Lumbar markers play a crucial part in the location of the center of rotation of the pelvic bone. An axis is drawn connecting both PSIS markers, and then another one connecting the Lumbar and Sacrum markers, the axis perpendicular to the coronal plane where the projections of these two axes meet goes through the pelvic center of rotation at the most posterior point of the bone, as it can be seen on ***Figure 7***. The right and left hip centers of rotation are located along the line that connects both great trochanter markers at a pre-set distance of ¼ of the total hip distance from the center of the segment to each respective side of the body.

The coordinate system associated with the pelvis was then defined as: the X axis (parallel to the line that connects both great trochanter markers and pointing in the lateral direction of the side that is being evaluated), the Z axis (perpendicular to the X axis and perpendicular to the axis connecting the Lumbar and Sacrum markers) and the Y axis (perpendicular to the X and Z axes). This coordinate system is shared by the entire pelvic rigid body that contains the markers shown in ***Figure 7*** and the pelvic center of rotation (purple cross in ***Figure 7***).

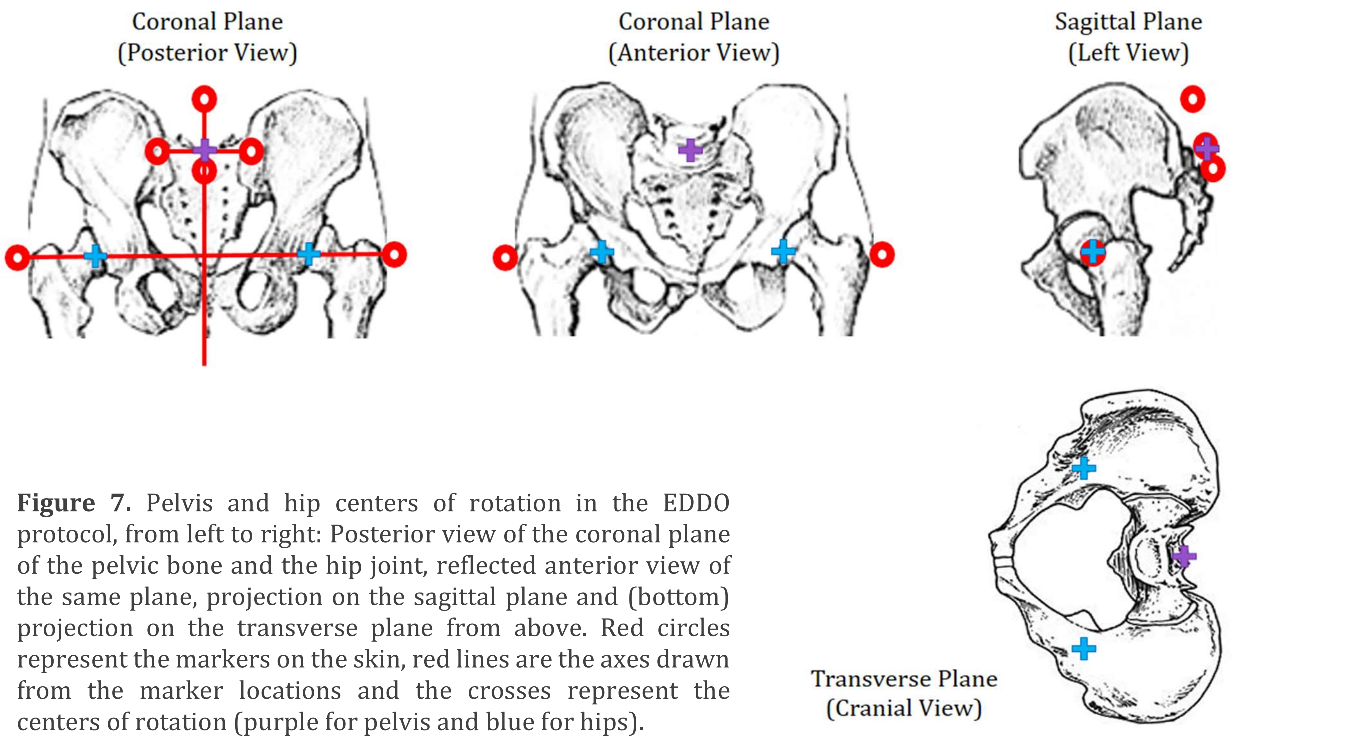

Figure 7. Pelvis and hip centers of rotation in the EDDO protocol, from left to right: Posterior view of the coronal plane of the pelvic bone and the hip joint, reflected anterior view of the same plane, projection on the sagittal plane and (bottom) projection on the transverse plane from above. Red circles represent the markers on the skin, red lines are the axes drawn from the marker locations and the crosses represent the centers of rotation (purple for pelvis and blue for hips).

After the location of the hip centers of rotation as explained on ***Figure 7***, the knee and ankle centers of rotation need to be located as well. To do this, the model creates a line connecting the hip center of rotation to the ankle marker of the same side, which becomes the main leg axis (purple segment in ***Figure 8***), then uses this leg axis and the pelvic Z axis to obtain a leg plane (purple axis in ***Figure 8***) onto which the knee and ankle markers are projected as shown on ***Figure 8***, these projections represent the knee and ankle joint centers of rotation, respectively. After the projections are obtained, the model computes the local femur and tibia Z axes by obtaining the perpendicular vector to the segment that joins the great trochanter markers and the segment that joins the hip center of rotation to the knee marker (green axis in ***Figure 8***).

The EDDO protocol performs a femur and tibia calibration in order to create a rigid body to represent the femur and tibia bones using the hip center of rotation and the markers in the thigh, knees and feet, this is done to obtain the coordinate axes for the remaining joint rotation centers (hip, knee and ankle).

The biomechanical model creates a matrix from the available axes and points so it can be used as an approximation to the final coordinate set of axes for the hip center of rotation. The matrix is formed by a segment drawn from the knee marker to the hip center, a segment drawn from the knee marker to the thigh marker, and the hip center itself (green segments and blue cross in ***Figure 8***). Then, the lowest point of this matrix (which is the knee center of rotation) is used for the computation of the final Y axis along with the hip center and subsequently, the final Y axis and the segment Z are used to obtain the final X axis (slightly tilted coordinate axes for the hip in ***Figure 8***). The same process is repeated for the tibia, resulting in the slightly tilted coordinate axes for the knee in ***Figure 8***.

Finally, a new rigid body is created for the foot, using the foot and ankle markers, and the matrix is constructed using the ankle center of rotation. The resulting coordinate system is shown on ***Figure 8*** as the ankle set of coordinates.

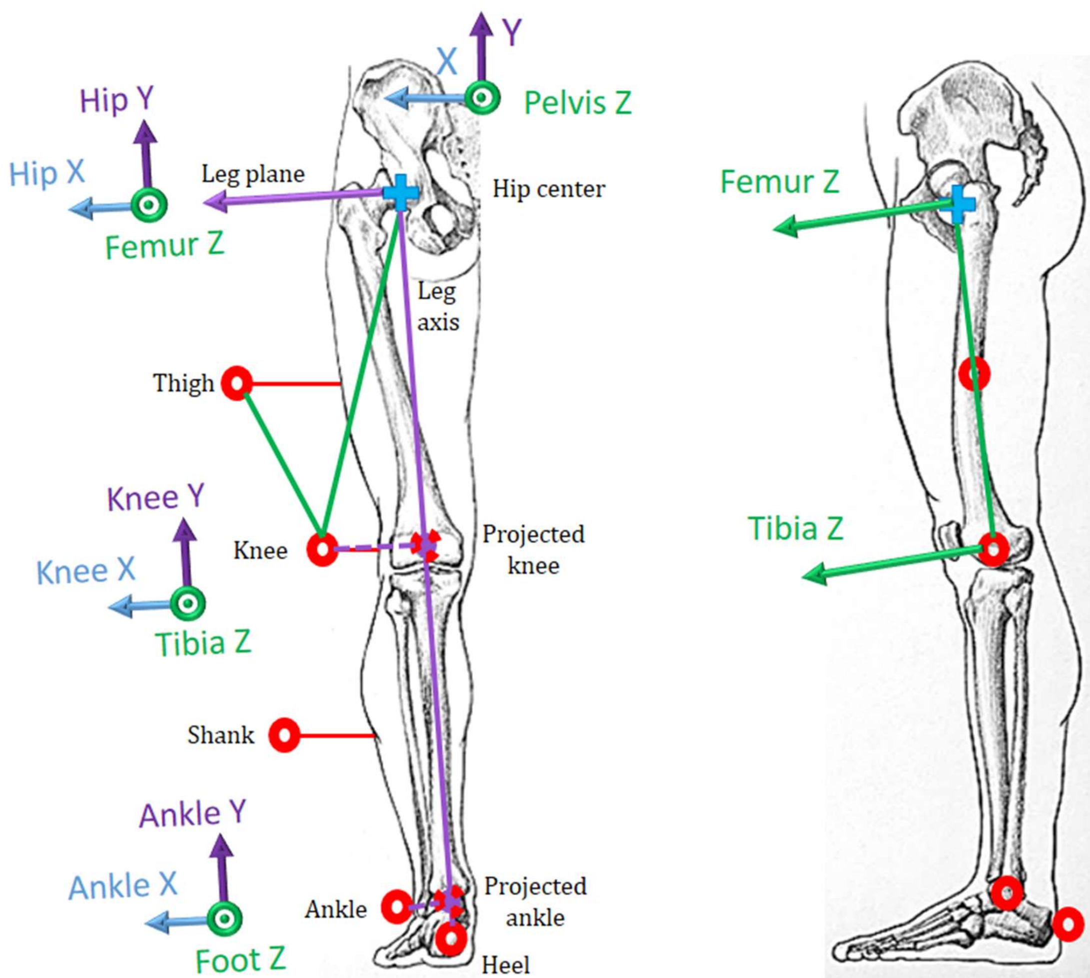

Figure 8. Hip, knee and ankle centers of rotation and associated coordinate systems. Markers in red. Left: Coronal plane view. Right: Sagittal plane view.

After the completion of the biomechanical model calculations, the coordinate systems and centers of rotation for the EDDO Protocol are as shown on ***Figure 9***, these are used to measure the final angles displayed on ***Table 6***.

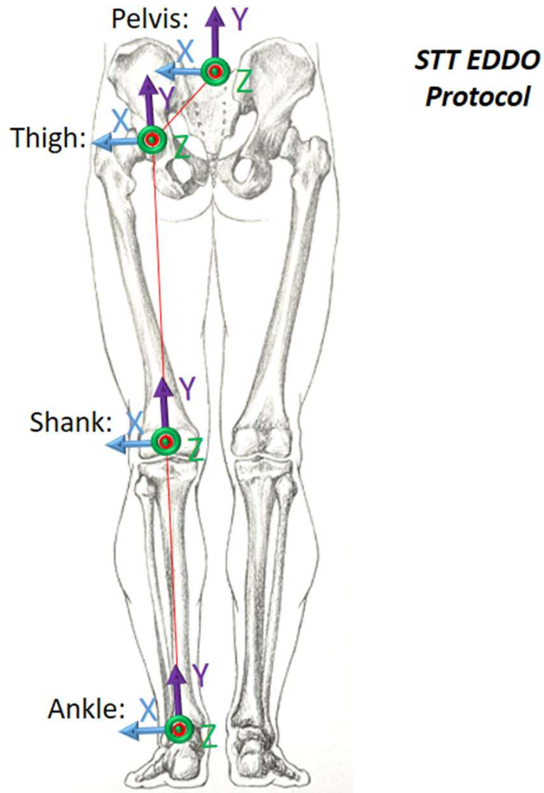

Figure 9. Coordinate systems for the EDDO Protocol. The red circles represent the anatomical centers of rotation of each joint and the axes represent the coordinate system associated with them and their orientation from a posterior view.

Table 6. Measured angles on the EDDO Protocol

Joint	Angle	Angle Measured Between	On Plane
PELVIS	Tilt	Global Y and Pelvic Y	Global X
	Obliquity	Global Y and Pelvic Y	Global Z
	Rotation	Global Z and Pelvic Z	Global Y
HIP	Flexion	Pelvic Y and Thigh Y	Pelvic X
	Add-Abduction	Pelvic Y and Thigh Y	Pelvic Z
	Rotation	Pelvic Z and Thigh Z	Pelvic Y
KNEE	Flexion	Thigh Y and Shank Y	Hip X
	Varus-Valgus	Variable due to singularity	
	Rotation	Thigh X and Shank X	Hip Y
ANKLE	Flexion	Shank Y and Ankle Y	Knee X
	Inv-Eversion	Shank X and Ankle X	Knee Z
	Rotation	Shank Z and Ankle Z	Knee Y
FOOT	Rotation	Global Z and Ankle Z	Global Y

5.4. Knee Singularity Problem Resolution

One of the main differences in the joint angles when comparing walking and running gait is the knee flexion. During walking the knee normally flexes up to 70°, however, when running it can reach a flexion of over 90°, which poses a conflict for the definition of the knee rotation along the global X axis (Knee Varus/Valgus). A graphic description of the knee singularity problem is presented on ***Figure 10***, ***Figure 11*** and ***Figure 12***.

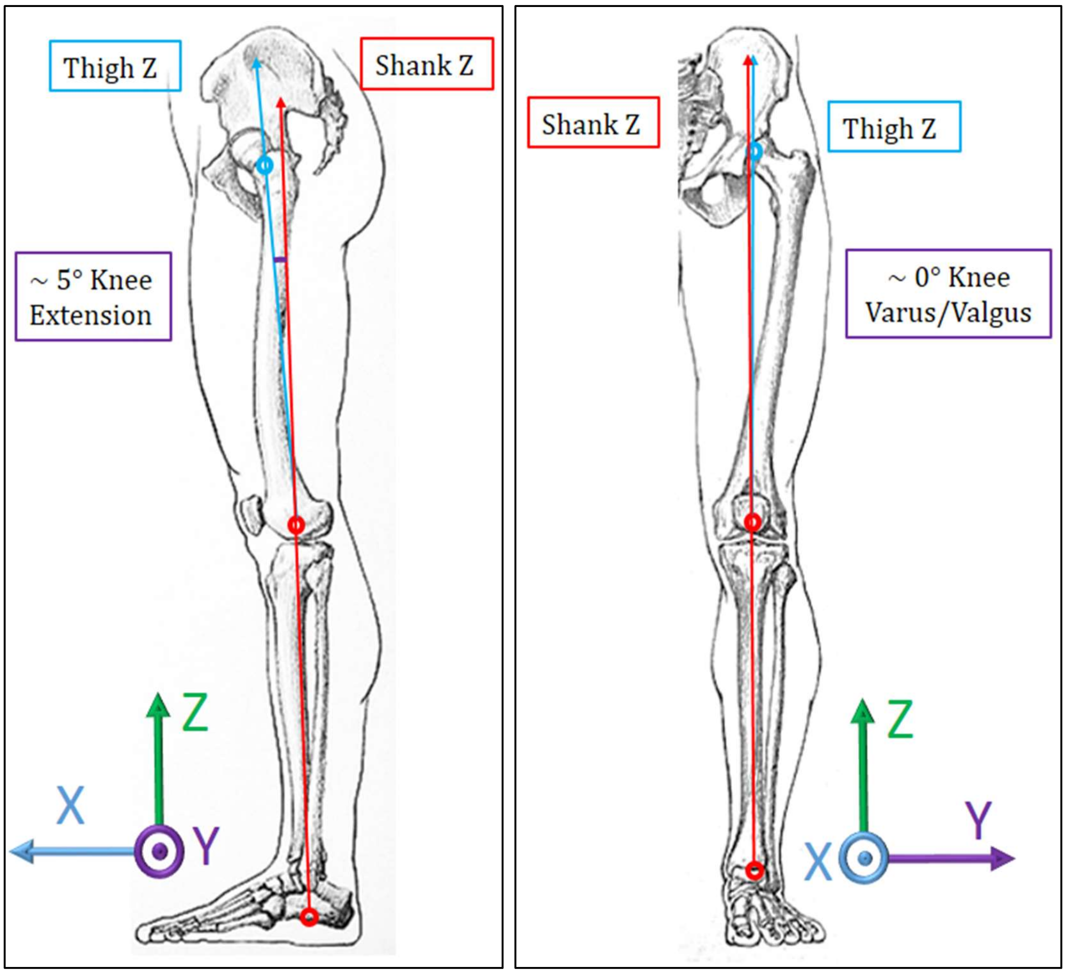

Figure 10. Thigh and shank axes in extended knee joint. Left: Sagittal view. Right: Coronal view.

The starting point of the knee angles at anatomical position are illustrated on ***Figure 10***. In the sagittal view (left), the flexion/extension of the knee is calculated by measuring the angle between the thigh Z axis and the shank Z axis. The knee varus/valgus is calculated using the same axes but from the coronal plane (right).

At 0° knee flexion/extension, the knee has a very limited range of motion in the remaining two dimensions due to the anatomy of the joint, however, when the knee flexion increases, the joint is able to rotate along the coronal plane, introducing varus/valgus as depicted on ***Figure 11***. During walking, the knee can rotate up to around 15° of varus (-) or 10° of valgus (+), generally after toe-off (at 70% of the gait cycle) when the knee flexion peaks at usually 70° (Le Borgne & Bontempi, 2013).

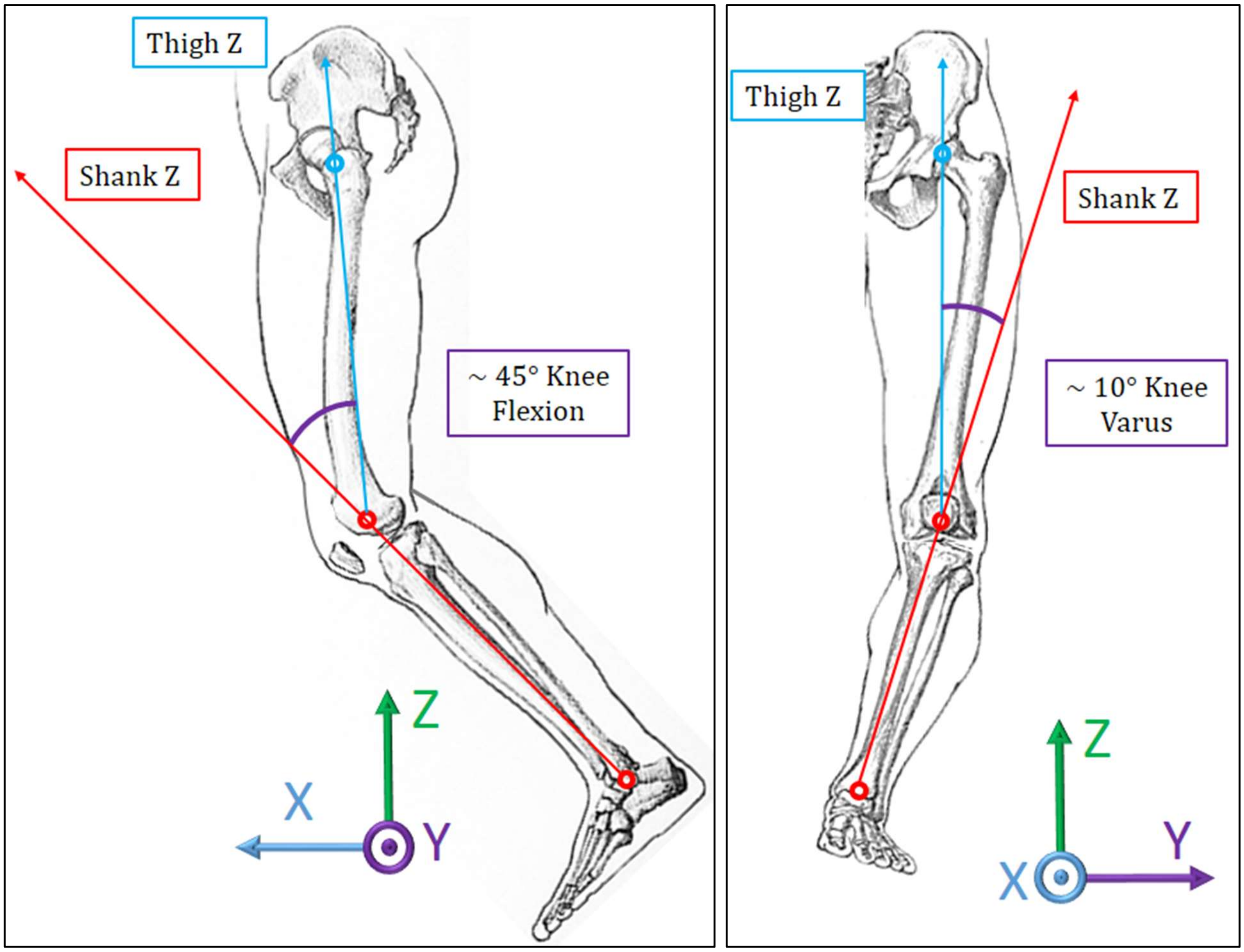

Figure 11. Thigh and shank axes in slightly flexed knee. Left: Sagittal view. Right: Coronal view.

It is usual that during walking, the highest knee flexion reached by the subject is 70° but in the case of running, knee flexion surpasses 90° during the mid-swing phase of the stride, which is a singular position for the knee joint. When the knee is flexed at 90°, the shank Z axis used to measure the varus/valgus projects on the coronal plane as a single point, making it impossible to measure the angle (as shown on ***Figure 12***), or as a perpendicular axis to the thigh Z, which yields an incorrect angle measurement for varus/valgus. In order to solve the previously explained problem, the biomechanical model redefines the calculation of knee varus/valgus as it is detailed in this section.

When the knee is flexed at 90°, the true varus/valgus can be measured by projecting the shank Z to a different plane, such as the transverse plane, and measuring the angle between this projection and the thigh X instead of the thigh Z (***Figure 12***, bottom).

In order to create a unique definition of knee varus/valgus that accurately defines the angle in all positions, a function was created to compute a weighted average of both angles (as seen from the coronal plane and from the transverse plane) depending on the knee flexion angle. The function used was:

$$weigh \quad \frac{e^{4(minimum\ module\ of\ the\ projected\ vectors\ to\ the\ plane} - 1}{e^4 - 1}$$

In which the minimum module of the projected vectors to each the coronal and transverse plane was calculated and each yielded a weight value that was used to multiply it by the angle between said vectors on the same plane. This operation results in exponentially smaller numbers as the vector projection decreases (the projection gets shorter when the movement approaches joint singularity), giving an exponentially more significant weight to the complementary angle, as seen from the other plane (evading the singularity measure). The result of adding the previous weighted angles is then divided by the cumulative sum of the computed weights in order to rescale to a measurement in real degrees.

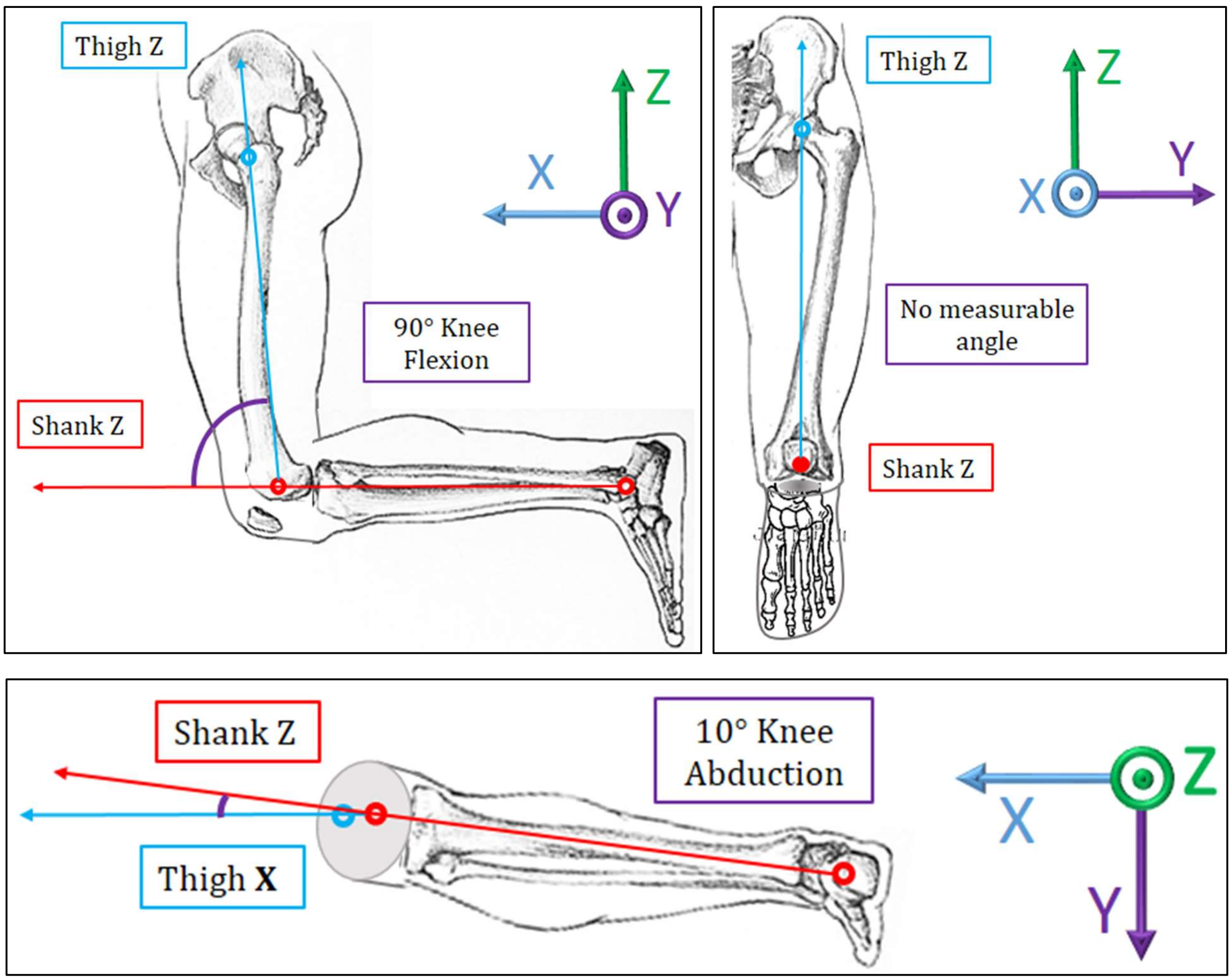

Figure 12. Thigh and shank axes in 90° flexed knee. Top left: Sagittal view. Top right: Coronal view. Bottom: Transverse view (from above).

The use of this adaptation aims to correct the knee singularity problem by defining its local coronal plane rotation as a compound rotation in both the local coronal plane and the local transverse plane, giving priority to the former when the knee is only slightly flexed and to the later when the knee is more pronouncedly flexed.

6. DATA COLLECTION

6.1. Equipment Setup

The subject tests were conducted in the data collection area in STT Systems. The setup of the equipment was parameterized as much as possible in order to maximize the capture capacity of the software and hardware, to do this, test trials were conducted beforehand and the results were revised to guarantee their suitability.

Once the results of the test trials were deemed appropriate, the correct placement of the equipment was marked on the floor using tape (for the portable system and the treadmill, which were the two elements that had to be moved in and out of the capture area in between trials or patients). A schematic of the distribution of the equipment in the testing area is shown in the figure below.

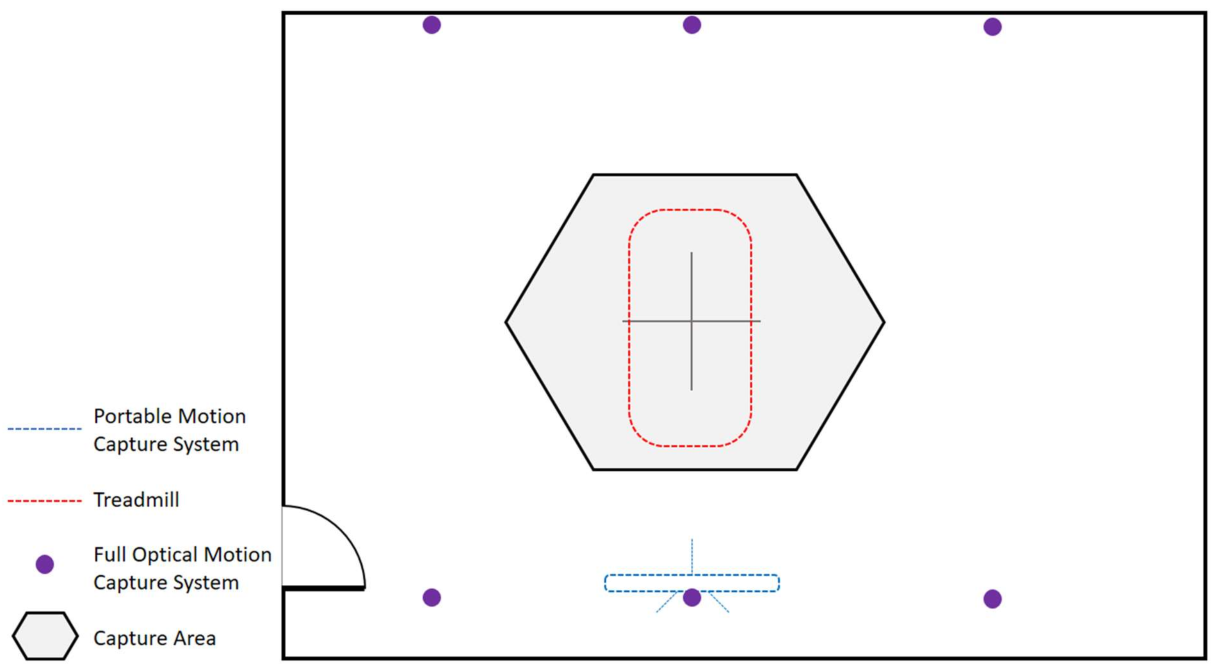

Figure 13. Diagram of the capture area with the defined positions of the equipment. Dotted lines represent the devices that have to be moved and where the tape was set on the ground to indicate their position.

The complete capture area within STT Systems is shown on ***Figure 13***, the system was used with the most recent valid calibration for each patient and the capture area did not change throughout the trials.

6.2. Data Collection Protocol

A total of 4 tests were performed by the 5 subjects, encompassing data collected with two protocols (STT HH and EDDO), two motion capture systems (full and portable), two types of surface (overground and treadmill) and two types of test (normal speed walking and light running). The data collection protocol followed for all subjects is described in ***Table 7***, as well as the distribution of the data obtained:

Table 7. Data collection procedure per subject

	Protocol	MoCap System	Surface	Test Type	Trials Acquired
Setup	*Marker placement (Helen Hayes Protocol)*				~
Test 1	Helen Hayes	Full System	Overground	Walking	5 (1 per subject)
Setup	*Portable system placement in the marked area* *Marker placement (EDDO Running Protocol)*				~
Test 2	EDDO Running	Simultaneous	Overground	Walking	40 (5 per MoCap, 4 repetitions)
Setup	*Treadmill placement in the marked area*				~
Test 3	EDDO Running	Simultaneous	Treadmill	Walking	10 (5 per MoCap)
Test 4	EDDO Running	Simultaneous	Treadmill	Running	10 (5 per MoCap)

6.3. Marker Placement

Another important aspect of the testing procedure was the marker placement on the subjects. In order to avoid error due to the misplacement of the markers, a standardized guide was designed and followed for each protocol in all of the tested subjects. The guide is presented in ***Table 8*** and ***Table 9***:

Table 8. Marker placement guide for Helen Hayes

STT Helen Hayes Protocol (Front View)

Sacrum at L5

Right Anterior Superior Iliac Spine on the palpable bone

Left Anterior Superior Iliac Spine on the palpable bone

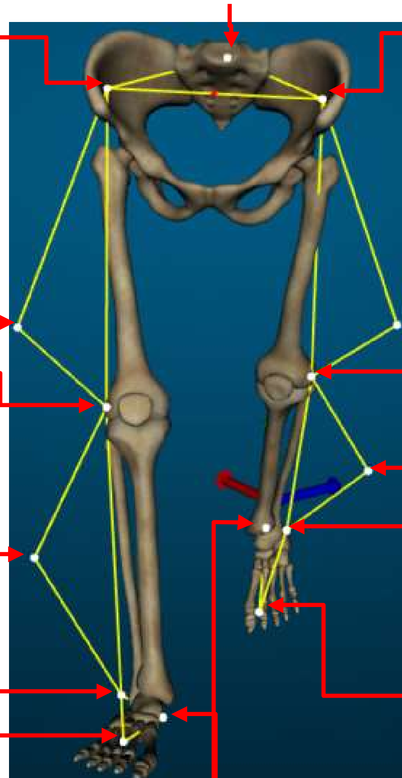

Right Thigh in the approximate middle of the thigh segment with an extensor bar for visibility

Left Thigh in the approximate middle of the thigh segment with an extensor bar for visibility

Right Knee on the palpable lateral femoral epicondyle

Left Knee on the palpable lateral femoral epicondyle

Right Shank in the approximate middle of the shank segment with an extensor bar for visibility

Left Shank in the approximate middle of the shank segment with an extensor bar for visibility

Left Ankle on the palpable lateral malleolus

Right Ankle on the palpable lateral malleolus

Left Toe on the juncture between second and third toe by the second phalange

Right Toe on the juncture between second and third toe by the second phalange

Right and Left Heels on the palpable balls of the respective calcaneus

Table 9. Marker placement guide for EDDO Running

EDDO Running Protocol (Back View)

Lumbar at L1

Left Posterior Superior Iliac Spine on the palpable bone

Right Posterior Superior Iliac Spine on the palpable bone

Sacrum at L5

Left Greater Trochanter on the palpable ball of the femoral epiphysis

Right Greater Trochanter on the palpable ball of the femoral epiphysis

Left Thigh in the approximate middle of the thigh segment with an extensor bar for visibility

Right Thigh in the approximate middle of the thigh segment with an extensor bar for visibility

Left Knee on the palpable lateral femoral epicondyle with a short extensor bar for visibility

Right Knee on the palpable lateral femoral epicondyle with a short extensor bar for visibility

Left Shank in the approximate middle of the shank segment with an extensor bar for visibility

Right Shank in the approximate middle of the shank segment with an extensor bar for visibility

Left Ankle on the palpable lateral malleolus with a short extensor bar for visibility

Right Ankle on the palpable lateral malleolus with a short extensor bar for visibility

Left Lateral Heel in line with Left Ankle and Left Heel (90° angle)

Right Lateral Heel in line with Right Ankle and Right Heel (90°)

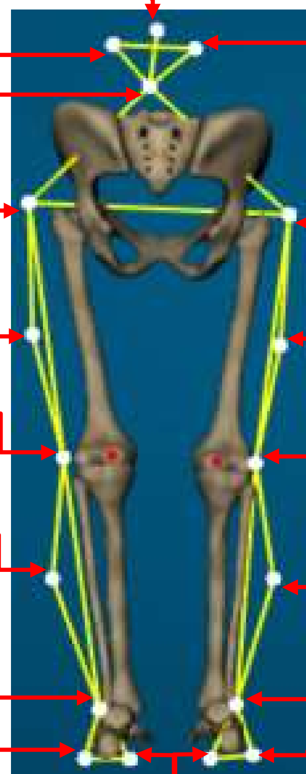

Left and Right Heels on the palpable ball of the calcaneus

The guides above were designed based on the location assumptions made on the source code for both protocols, ensuring that the biomechanical model will process the marker data that truly corresponds to the anatomical locations where they should be placed. Since all markers are identical and the order in which they are placed on the subject does not alter the final result as long as the entire set is placed, no other clarifications to the placement of markers was needed for the experimental setting.

7. COMPARATIVE ANALYSIS

7.1. Comparison Software

In order to analyze the resulting data from the previously mentioned trials, it was imperative to replicate part of the functionalities of the STT Clinical 3DMA software such as stride selection within a trial and the creation of graphs representing the behavior of each joint during the gait cycle. In addition to this, a tool for trial merger and another for comparative plotting were developed. The complete data processing flowchart is explained in the following section and copies of the MATLAB programs and functions are attached as an appendix.

7.1.1.Data Processing Flowchart

DATA CAPTURE

All data was captured with STT Systems software in the STT's data collection area.

↓

DATA IMPORT

CSV Files — One for each joint (pelvis, hip, knee, ankle, foot). The file contains the angle value of the joint in all three dimensions throughout the time of the trial in seconds.

TXT File — One per trial. The file contains the automatically detected events of the gait cycle (such as toe-off, heel strike) and their respective time within the trial.

↓

STEP IDENTIFICATION

StepID.m — This function goes through the event names (imported from the TXT File), locates all events named 'initial contact' (which is the starting point of every step) and saves an array of their corresponding times for left and right foot.

↓

STEP SEPARATION

StepSeparationInterp.m — This function goes through the array of step start times, finds the values within the trial for each angle measured and splits the original trial array at each of these points, saving each section as a complete step. Each of the separated steps is then lineally interpolated assuming the start of the step as 0% of the gait cycle and the end as 100% (in 1% intervals).

↓

STEP FILTERING

StepsFilterStd.m — This function uses a threshold to eliminate steps from the step array, the standard deviation of the step data is compared to the threshold and eliminated if higher, this effectively subtracts the steps that contain capture data error (standard deviation of thousands of degrees).

StepsFilterSelection.m — This function goes through the step array plotting the remaining steps one by one and allowing the user to select which steps should be kept in the trial and which should be eliminated (for the steps that are within the standard deviation threshold but still present error or noise).

STEP COMBINATION

mergeTrials.m — This function appends steps of different trials together in order to obtain a more sizeable sample of steps for the final combination.

StepsUnif.m — This function goes through the step array and computes the mean and standard deviation of the angle for each interval of the gait cycle. The final results can be plotted in order to compare them with standard gait curves.

CURVE PLOTTING

plotCurves.m — This function plots curves for the inputted trial: Right and left side plots with one curve (mean and deviation) for each angle measured per joint.

plotCurves2.m — This function plots curves for the 2 inputted trials: Right and left side plots with 2 curves (mean and deviation) for each angle measured per joint.

plotCurves3.m — This function plots curves for the 3 inputted trials: Right and left side plots with 3 curves (mean and deviation) for each angle measured per joint.

7.1.2.Curve Comparison

After the data from the trials is processed, the plotting tools allow for the creation of comparative reports, which contain the overlapped graphs from the desired trials and their respective step statistics. An example of the resulting plots is shown on ***Figure 14*** and ***Figure 15***, this is how the final results will be presented.

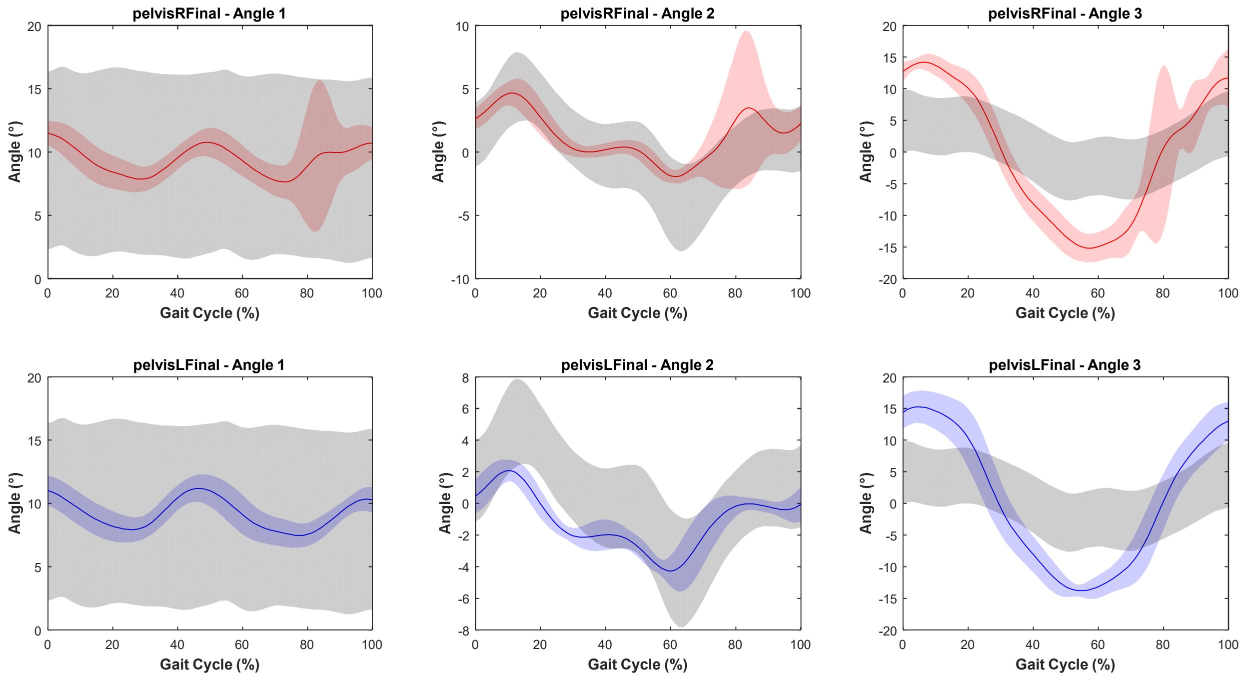

Figure 14. Sample of the resulting plots for the pelvic joint with one trial. First row (in red) represents the right leg side and second row (in blue) represents the left side, mean values in a solid line and standard deviation as a colored area. The first column shows the angle projected to the sagittal plane (in this case Pelvic Tilt), the second column shows the angle projected to the frontal or coronal plane (in this case Pelvic Obliquity) and the third column shows the angle projected to the transverse or horizontal plane (in this case Pelvic Rotation). The gray areas in all plots represent the normal data used as a baseline for the clinical reports in STT.

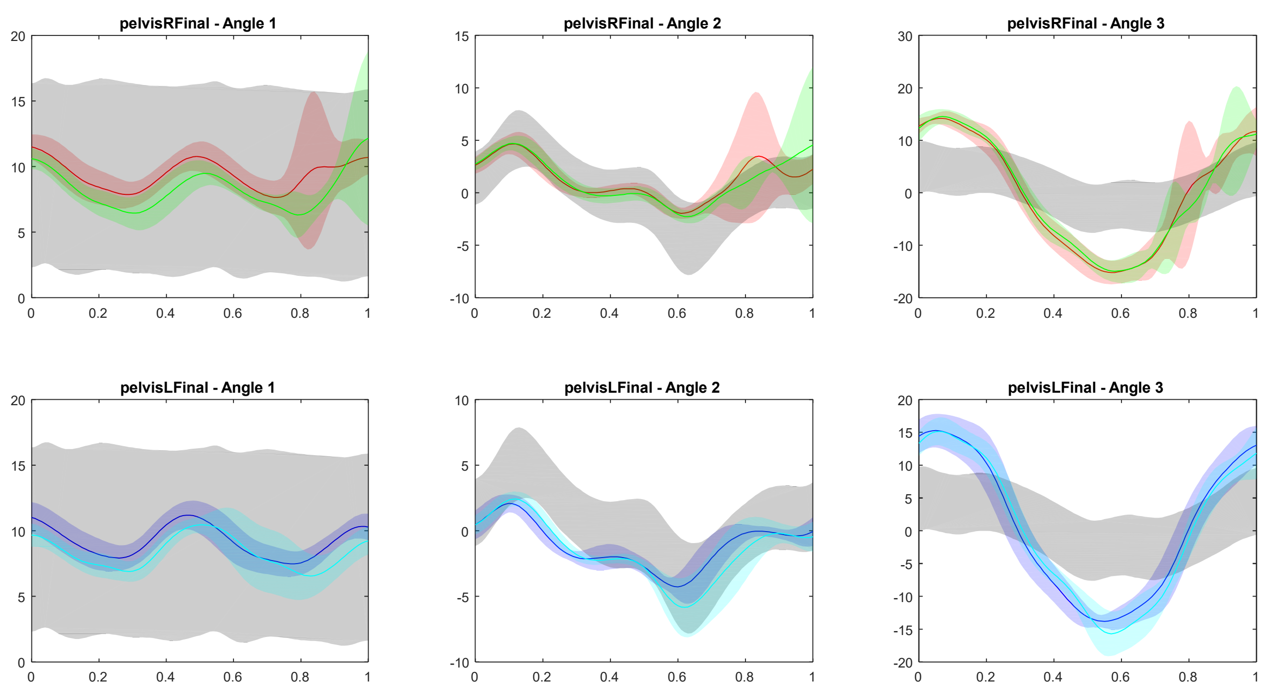

Figure 15. Sample of the resulting plots for the pelvic joint with two trials. In addition to the explanation in the figure above, these plots contain two curves, each representing one trial. The red and blue curves correspond to one of the trials, and the green and cyan curves correspond to the other one.

The visual representation of the results in the plots above greatly aided the early stages of the project since it was used to check the results of the test trials for the different protocols and forms of data acquisition, and understand the correlation of these variables in the final result. The data of the trials in the plots was also statistically compared in order to obtain quantitative results of the differences that could lead to conclusions in the validation process.

7.2. Numeric Data Comparison

Aside from the visual analysis of the results, some sort of numeric comparison was also needed in order to draw conclusions as to the significance of the visual differences observed on the plots. Two parameters were used to numerically compare the graphs: clinical assessment significance and presence of noise.

Clinical assessment significance refers to the necessary amount of degrees of difference between a set of plots in a particular region of the gait cycle that could significantly alter clinical assessment of the status of the subject. According to the literature, a 5° difference has been proven to start affecting the clinical assessment of the data (McGinley, Baker, Wolfe, & Morris, 2009).

Regarding the presence of noise, in the case of gait analysis there is a significant amount of noise that gets introduced due to the triangulation of the markers in the 3D space, meaning, the more angles of the capture area are available, the less chance of misplacement of the marker in the 3D space. The momentary misplacement of a marker in the 3D space translates graphically in a signal with repeated peaks in the mean and standard deviation. A sample comparison between data with noise and data without it is presented on ***Figure 16***.

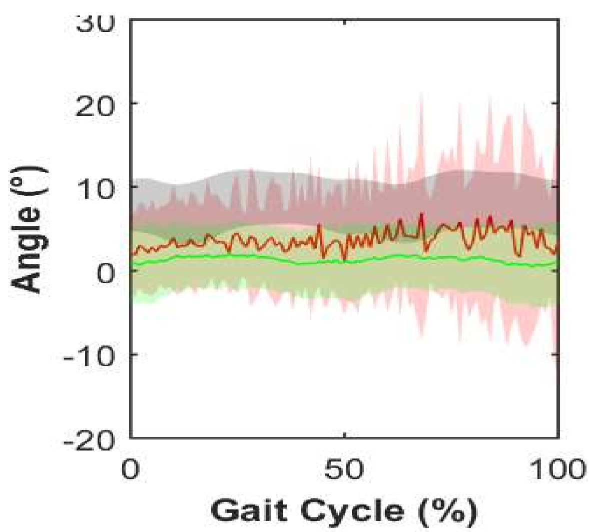

Figure 16. Presence of noise in sample data. Data without noise in green and data with noise in red. Solid lines represent the mean of the dataset and shaded areas the standard deviation.

8. RESULTS

The first step in the validation procedure was to analyze the collected data from the trials and segment it in order to isolate the individual parameter comparisons that conformed the final protocol comparison. The different parameter comparisons for each joint evaluated (right and left side of the pelvis, right and left hip, right and left knee and right and left ankle in all 3 main body planes) are shown in the following section. For every plot set in this section and the following, the top row represents the right side of the body and the bottom row represents the left, the 1st column represents the observed angle as seen from the Y plane of the joint (Tilt, Flexion), the 2nd column the angle as seen from the X plane of the joint (Obliquity, Adduction, Valgus, Eversion) and the 3rd column the angle as seen from the Z plane of the joint (Rotation). The normative curves are shown in gray.

8.1. Segmented Results by Motion Capture System

The first parameter to be examined was the influence of the motion capture system in the final data. As shown in ***Table 7***, tests 2, 3 and 4 were recorded using both motion capture systems simultaneously, the data from these tests was unified and is presented in the following figures. The next 4 figures represent the data from **Test 2***: Walking with the EDDO protocol overground*.

8.1.1. Results from Test 2

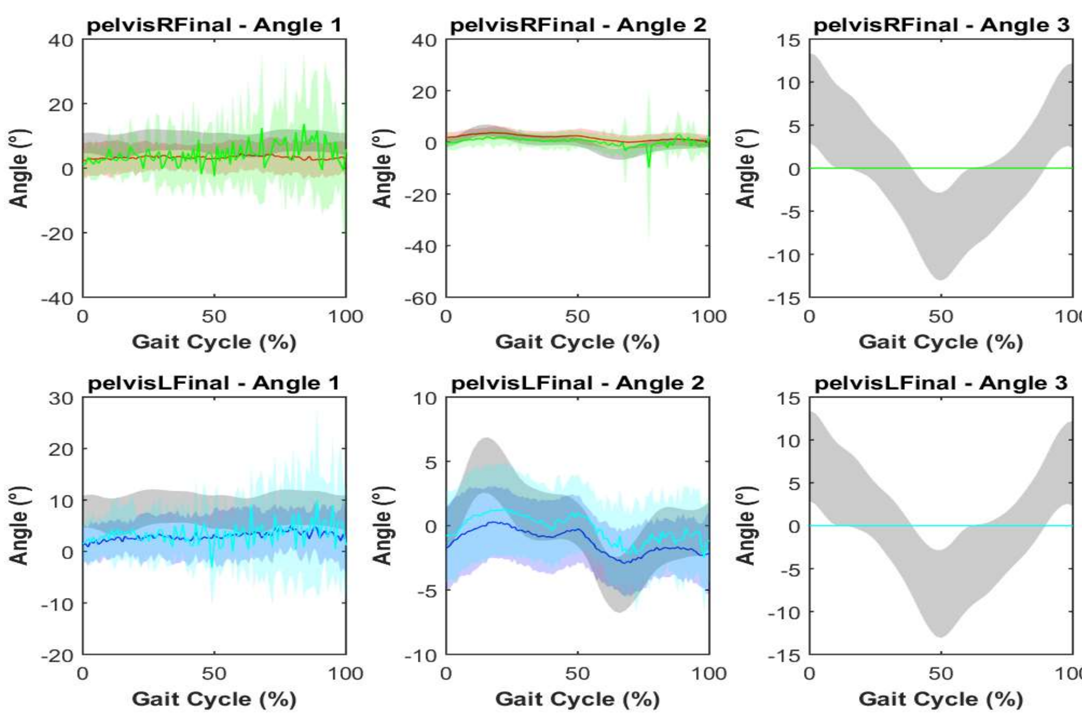

Figure 17. Motion Capture System Comparison for trials using the **EDDO protocol overground for the pelvic joint**. Red and blue plots represent the data from the Full Motion Capture System, and green and cyan represent the Portable Motion Capture System.

As shown in **Figure 17**, the EDDO protocol, unlike the Helen Hayes protocol, does not compute data for pelvic rotation due to the restrictive placement of its markers for the intended portable system visibility. This angle, plus the feet angles (for similar reasons), will not be taken into account for the following comparisons.

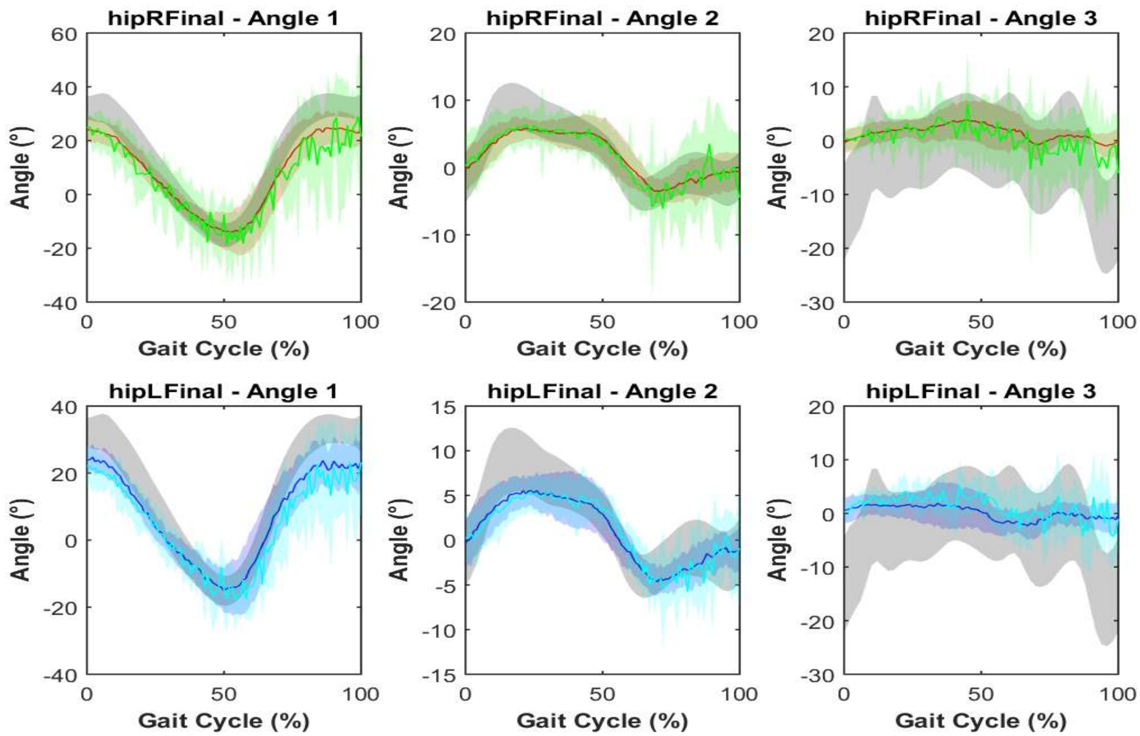

Figure 18. Motion Capture System Comparison for trials using the **EDDO protocol overground for the hip joint.** Red and blue plots represent the data from the Full Motion Capture System, and green and cyan represent the Portable Motion Capture System.

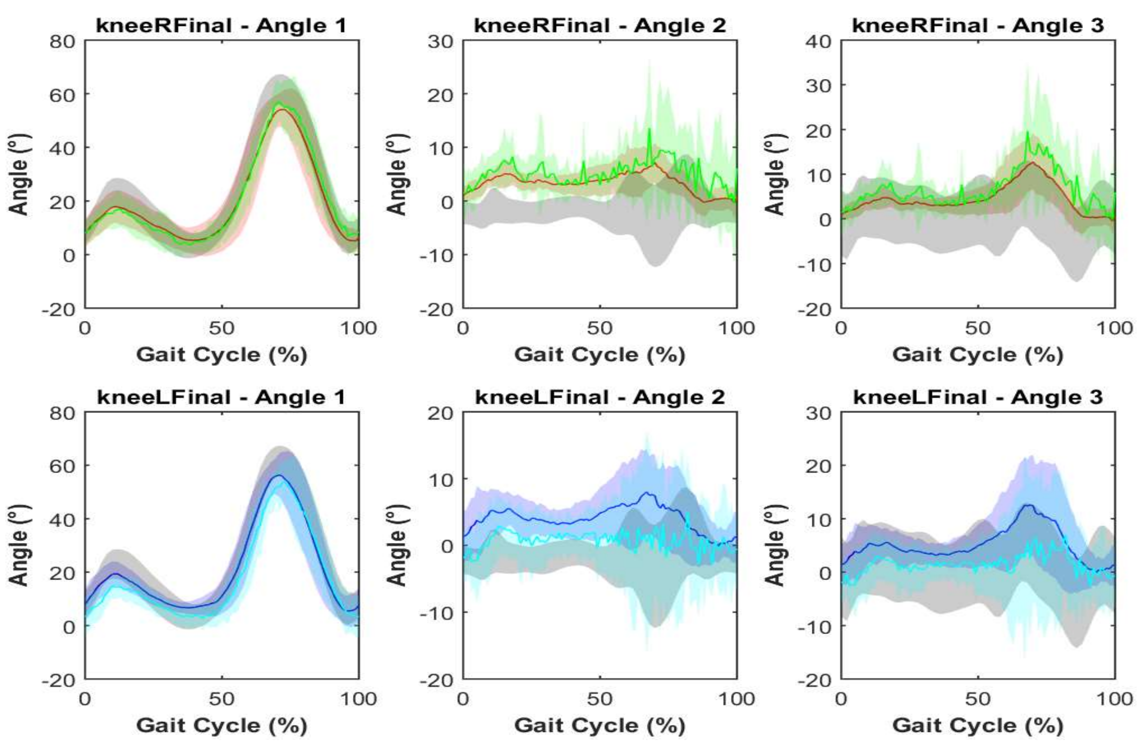

Figure 19. Motion Capture System Comparison for trials using **the EDDO protocol overground for the knee joint.** Red and blue plots represent the data from the Full Motion Capture System, and green and cyan represent the Portable Motion Capture System.

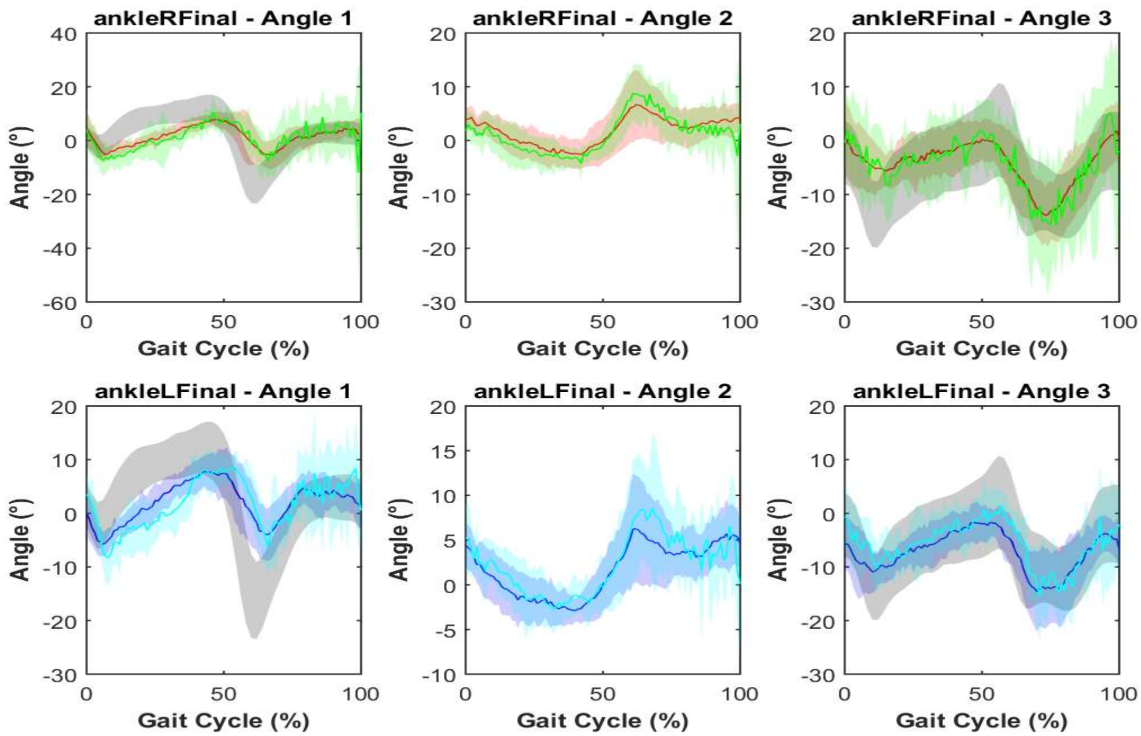

Figure 20. Motion Capture System Comparison for trials using **the EDDO protocol overground for the ankle joint**. Red and blue plots represent the data from the Full Motion Capture System, and green and cyan represent the Portable Motion Capture System.

One of the most notorious differences between the two sets of data displayed on the previous figures is that the data captured with the portable system (green and cyan in all plots) has slightly more noise alterations than the data captured by the full MoCap system. This increased noise was an expected result, since the visibility of the portable system is diminished as the subject walks further from the device, while the visibility of the full system (because of it being installed on the roof) remains quite similar as far as the subject walks inside the capture area.

The reason for the particularly notorious peaks of noise (as observed in the increased frequency of the maximum-minimum fluctuations of the signals when compared to the other sets of data) at the end of the gait cycle for the portable system data is that by the time the subject completed the second step walking away from the MoCap device, the distance between the device and the markers was great enough to generate a significant amount of noise in the capture.

However, apart from the slight increase of noise, the data from both motion capture systems overlaps almost identically in all joints and angles of observation, the knee varus/valgus and rotation on the left side (***Figure 19***) being the most notoriously different with an offset of less than 2°, which does not reach the 5° difference that has been proven to start affecting the clinical assessment of the data (McGinley, Baker, Wolfe, & Morris, 2009).

It is important to clarify that the ideal scenario for the use of the portable MoCap system is with a treadmill (as it was done for tests 3 and 4 of ***Table 7***), which makes it possible for the subject to remain at an optimal distance from the device during a full capture. The following figures show the results of **Test 3**: *Walking with the EDDO protocol on treadmill.*

8.1.2.Results from Test 3

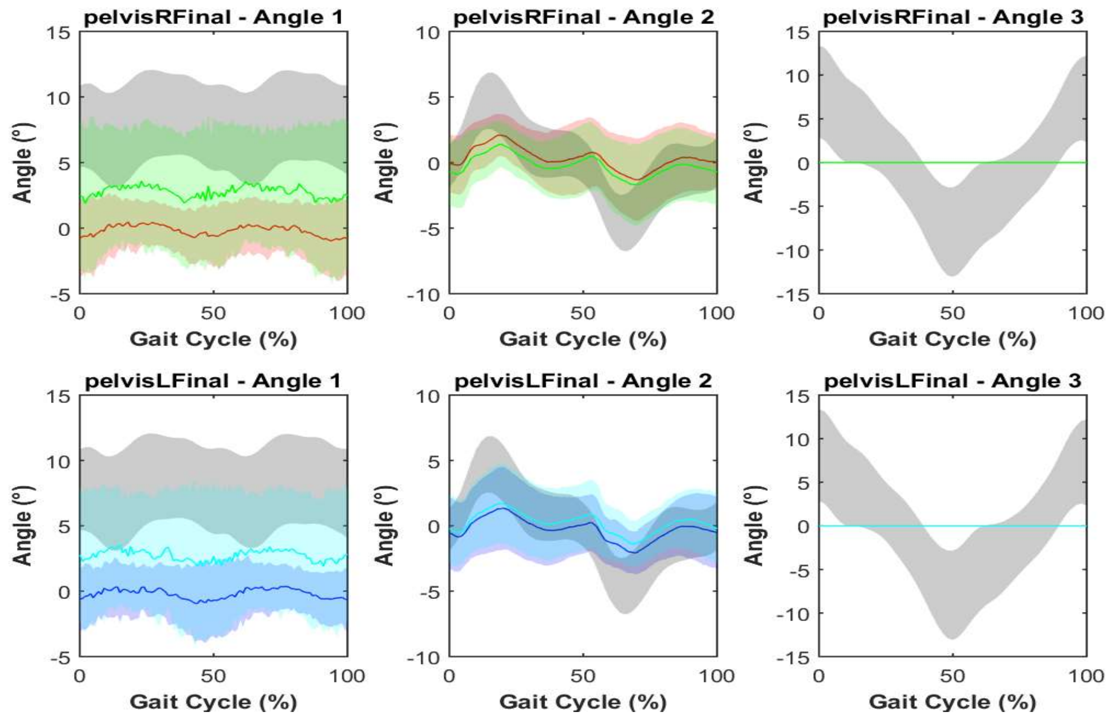

Figure 21. Motion Capture System Comparison for trials using the **EDDO protocol on treadmill for the pelvic joint**. Red and blue plots represent the data from the Full Motion Capture System, and green and cyan represent the Portable Motion Capture System.

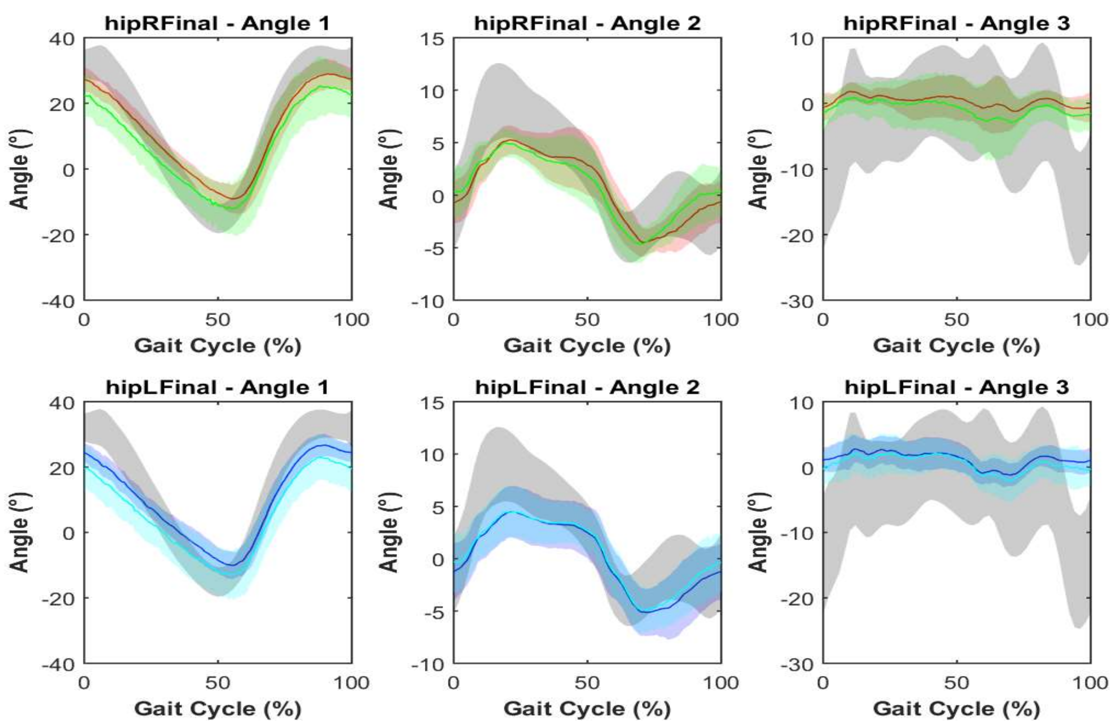

Figure 22. Motion Capture System Comparison for trials using the **EDDO protocol on treadmill for the hip joint.** Red and blue plots represent the data from the Full Motion Capture System, and green and cyan represent the Portable Motion Capture System.

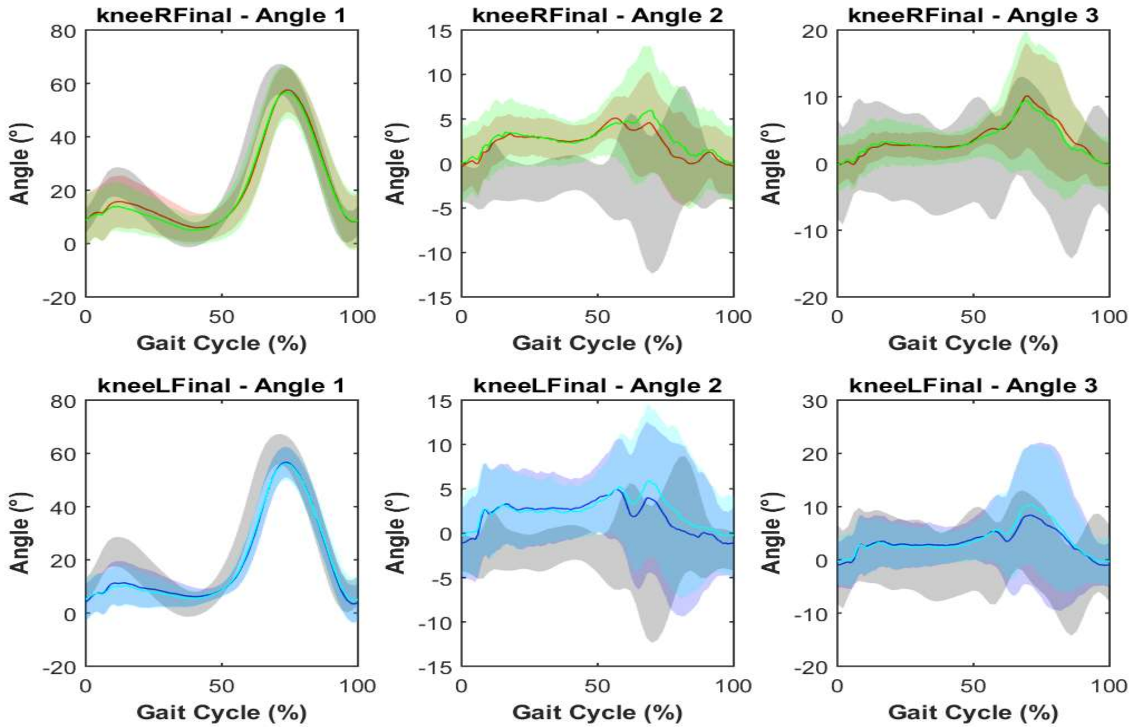

Figure 23. Motion Capture System Comparison for trials using the **EDDO protocol on treadmill for the knee joint.** Red and blue plots represent the data from the Full Motion Capture System, and green and cyan represent the Portable Motion Capture System.

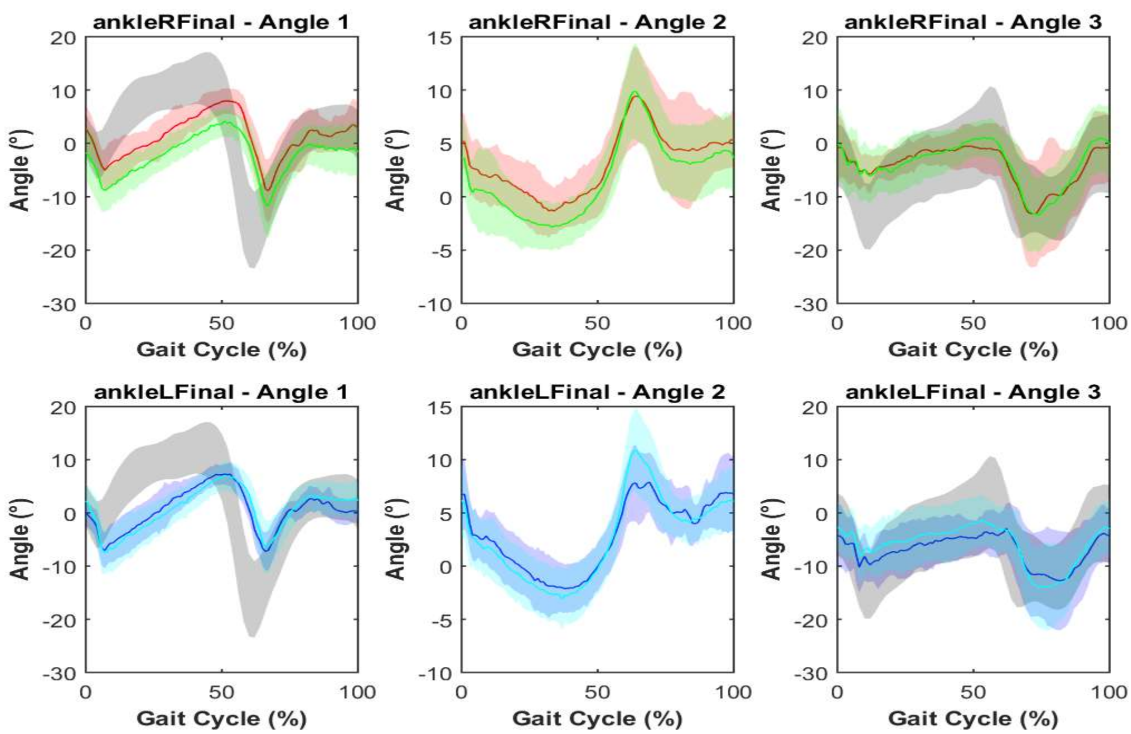

Figure 24. Motion Capture System Comparison for trials using the **EDDO protocol on treadmill for the ankle joint**. Red and blue plots represent the data from the Full Motion Capture System, and green and cyan represent the Portable Motion Capture System.

As it can be seen from the previous plots, the data from both motion capture systems contains less noise and remains with an almost identical overlap for all joints and angles.

The most significantly different sets of data in this case are the pelvic tilt plots (**Figure 21**), with an offset of approximately 2.5°, continuing to be similar enough to be deemed equivalent, and the ankle inversion-eversion plots where the peak right after toe-off (65% of the gait cycle) on the left side reaches 4° of inversion more for the portable system than the full system, which was caused by a momentary occlusion of the foot markers during that particular portion of the gait cycle along the trials. This systematic occlusion is not uncommon, since the ankle-foot section has a higher marker density and is known to cause labeling problems in the software.

The last simultaneous test to be performed in order to compare the motion capture systems was **Test 4**: *Running with the EDDO protocol on treadmill*. Results are presented in the following figures.

8.1.3.Results from Test 4

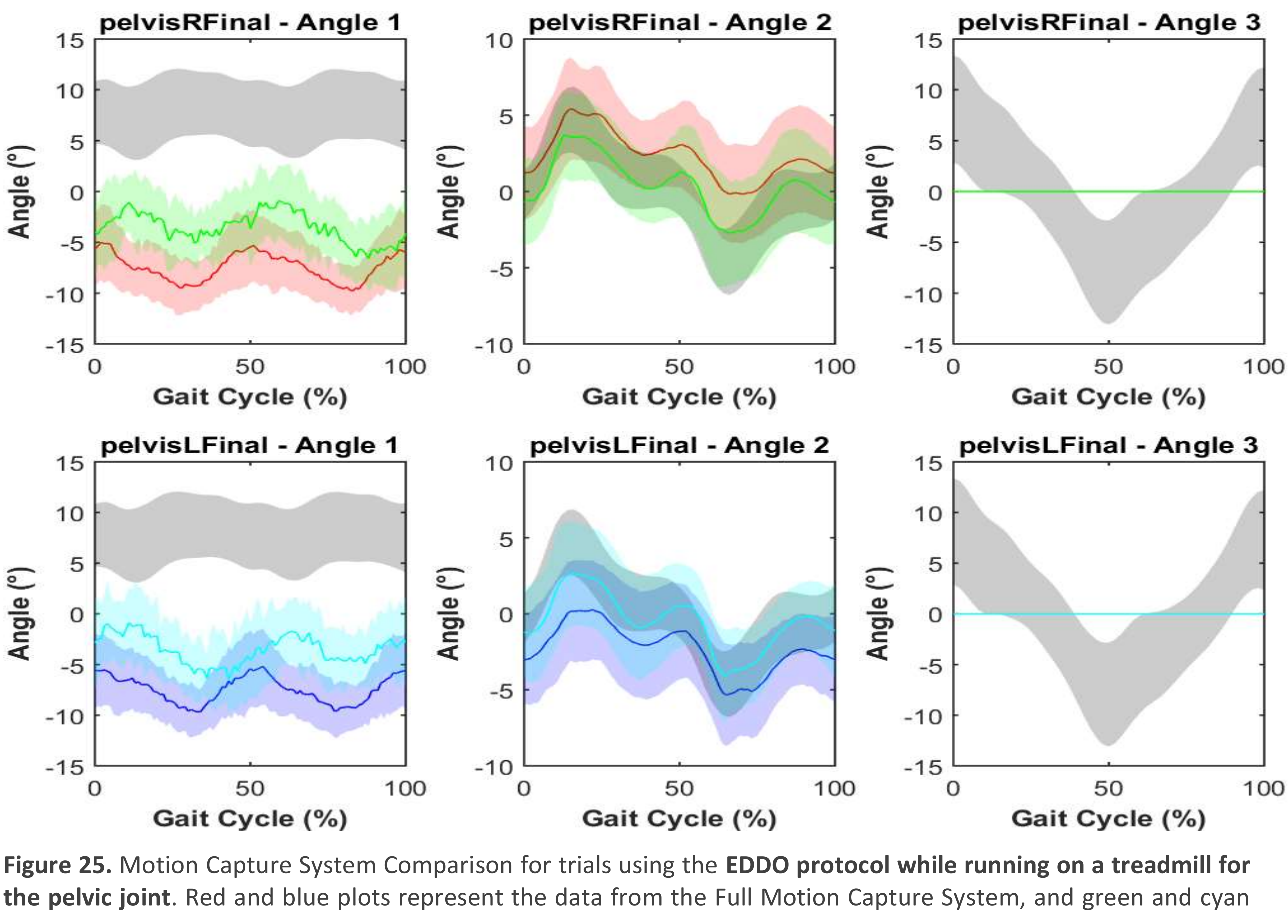

Figure 25. Motion Capture System Comparison for trials using the **EDDO protocol while running on a treadmill for the pelvic joint**. Red and blue plots represent the data from the Full Motion Capture System, and green and cyan represent the Portable Motion Capture System.

A reappearance of the noise was expected due to the increased vibrations caused by running on the treadmill, also, since the normative dataset being used to compare the plots is meant for walking gait, the results from running should further deviate from the gray curves for a few key plots, such as the pelvic obliquity in ***Figure 25***, which shows that the data from both motion capture systems undulates in a more pronounced way than the normative walking data displayed in gray.

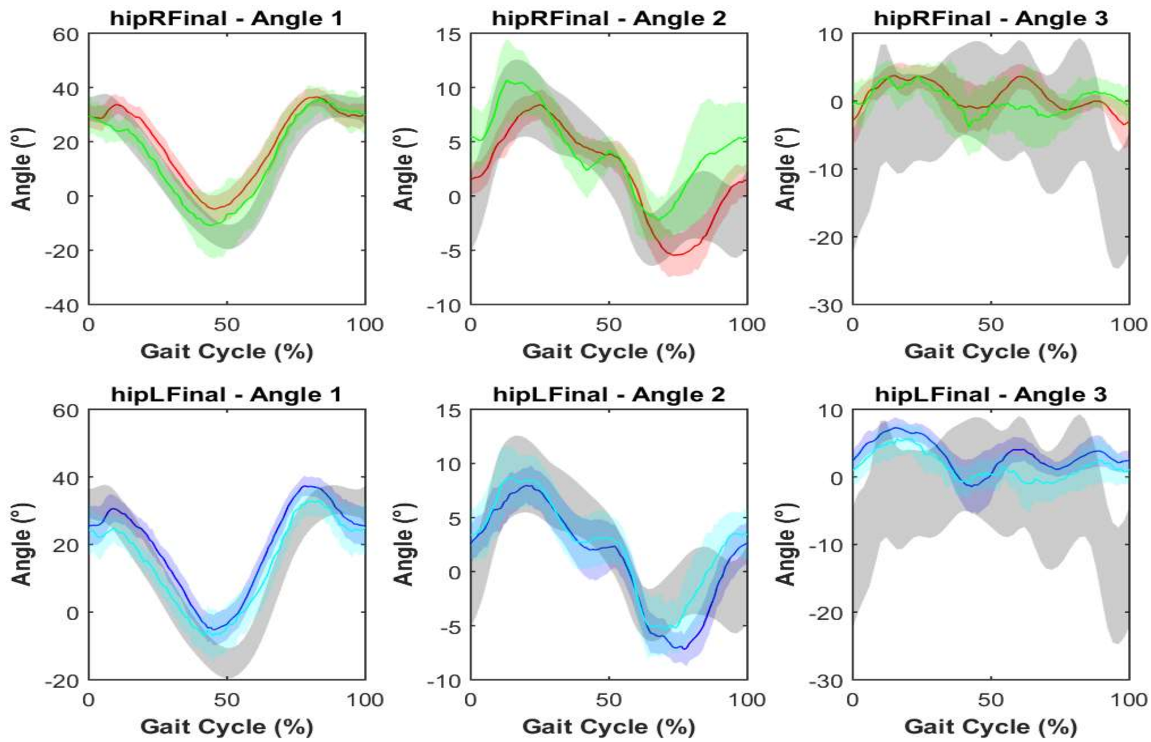

Figure 26. Motion Capture System Comparison for trials using the **EDDO protocol while running on a treadmill for the hip joint.** Red and blue plots represent the data from the Full Motion Capture System, and green and cyan represent the Portable Motion Capture System.

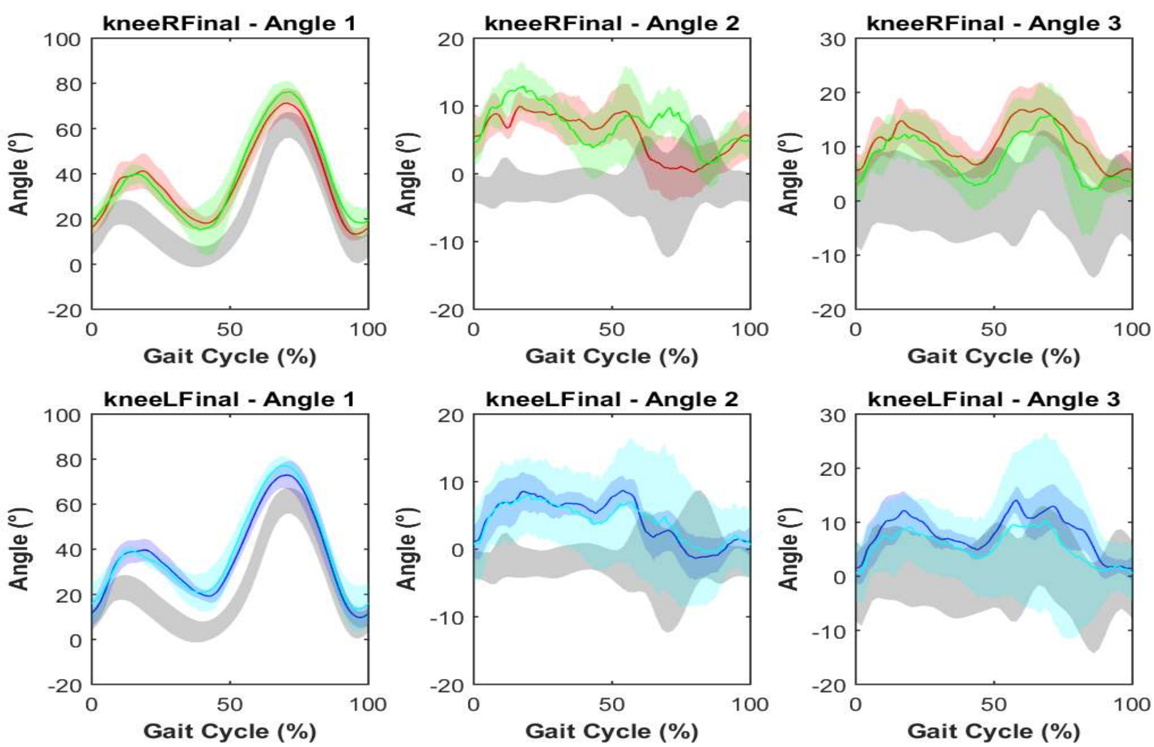

Figure 27. Motion Capture System Comparison for trials using the **EDDO protocol while running on a treadmill for the knee joint.** Red and blue plots represent the data from the Full Motion Capture System, and green and cyan represent the Portable Motion Capture System.

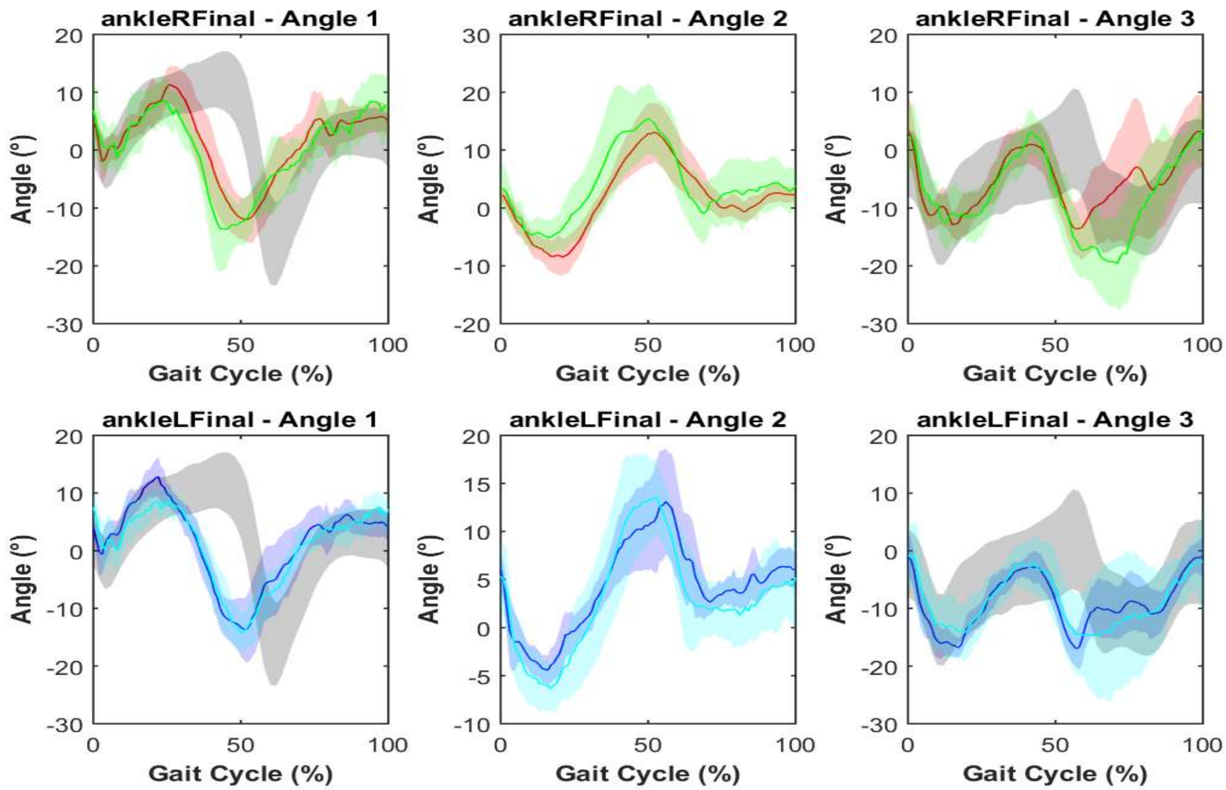

Figure 28. Motion Capture System Comparison for trials using the **EDDO protocol while running on a treadmill for the ankle joint.** Red and blue plots represent the data from the Full Motion Capture System, and green and cyan represent the Portable Motion Capture System.

After analyzing the data of the three simultaneous tests contained in ***Table 7***, no significant difference between the two motion capture systems was identified, since none of the plots showed a difference of over 5° in between them, the margin determined by the literature as the clinical assessment significance margin. Even though some of the plots shown above do not look exactly the same, the slight differences between systems identified on some joints and angles can be attributed to occlusions due to the different visibilities of both systems and none are greater than the range that compromises clinical analysis according to the literature.

8.2. Segmented Results by Walking Surface

The next parameter to be evaluated was the influence of a surface change when walking in order to identify the possible gait alterations when changing from walking overground to walking on a treadmill.

The literature reports mixed conclusions on expected changes when walking on a treadmill as opposed to walking overground. The main significant difference reported was a change in hip range of motion and on maximum hip flexion, as well as some cadence differences that were mostly due to a mismatch on overground and treadmill speeds (Alton, Baldey, Caplan, & Morrissey, 1998).

After concluding that the motion capture system does not significantly alter the collected data, all trials with overground walking were combined in order to compare them to all trials done walking on the treadmill. The results of the comparison are shown below for all joints and angles.

8.2.1. Results from Test 2 & 3

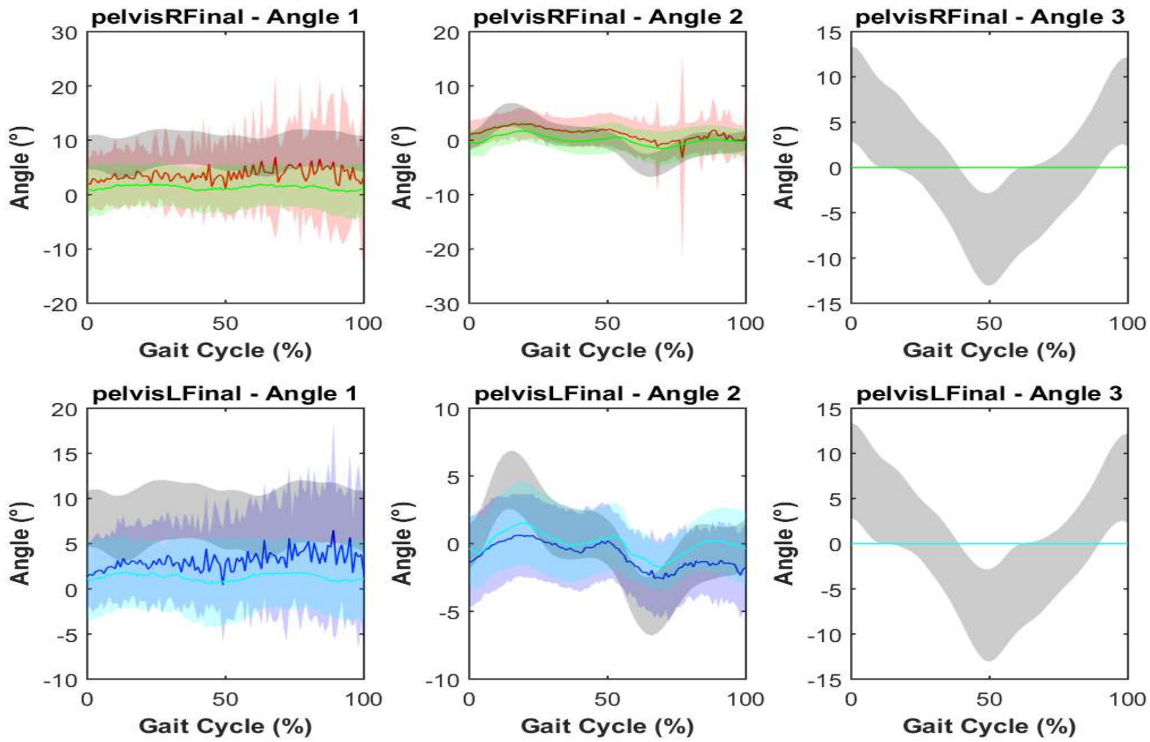

Figure 29. Walking Surface Comparison for trials using the **EDDO protocol for the pelvic joint.** Red and blue plots represent the data from the overground trials, and green and cyan represent the treadmill trials.

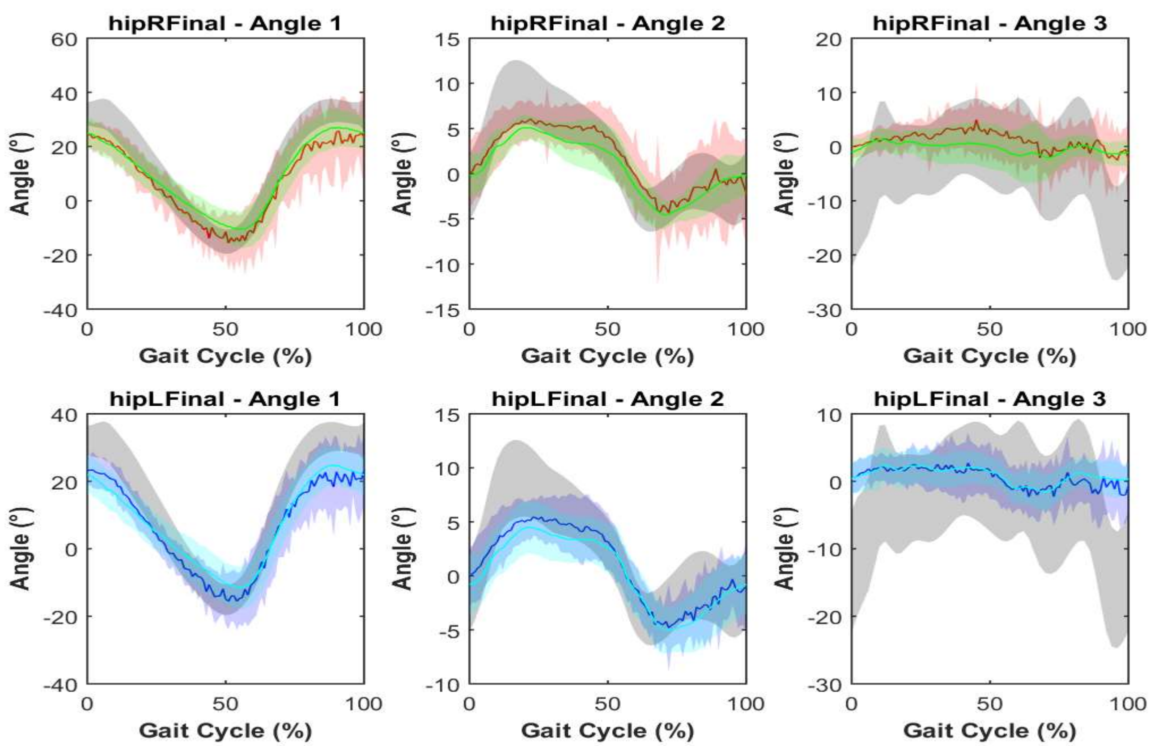

Figure 30. Walking Surface Comparison for trials using the **EDDO protocol for the hip joint.** Red and blue plots represent the data from the overground trials, and green and cyan represent the treadmill trials.

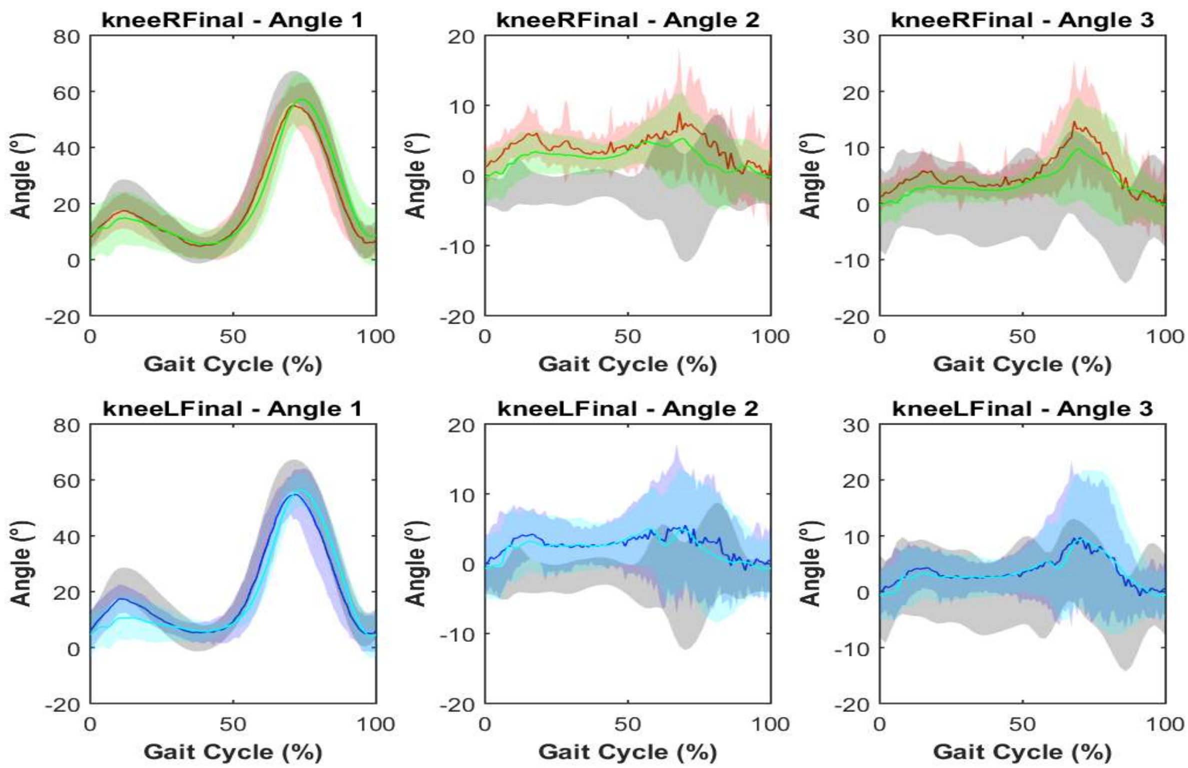

Figure 31. Walking Surface Comparison for trials using the **EDDO protocol for the knee joint.** Red and blue plots represent the data from the overground trials, and green and cyan represent the treadmill trials.

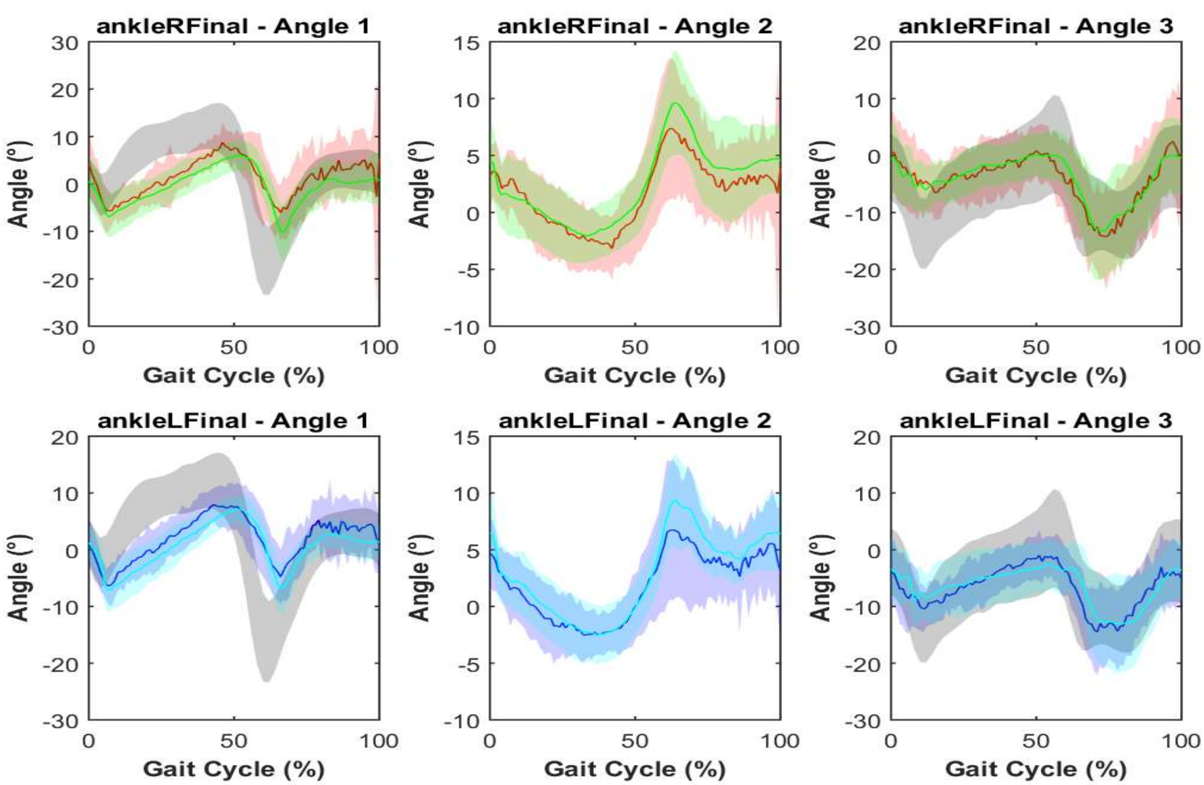

Figure 32. Walking Surface Comparison for trials using the **EDDO protocol for the ankle joint.** Red and blue plots represent the data from the overground trials, and green and cyan represent the treadmill trials.

As show on the previous plots, the incidence of the walking surface was not significant enough to show a drastic difference between the datasets. A few reasons that could explain why the present study slightly differs from the expected results from the literature are the subjects used for the trials. In all 5 cases, subjects were previously acquainted with the treadmill and the speed of their overground walking was carefully met on the treadmill in order to reduce discrepancies. However, since the literature reports significant differences only on hip flexion maximum and overall hip range of motion (Rozumalski, Novacheck, Griffith, Walt, & Schwartz, 2015), the present results agree with the past research for all other joints and angles in the study (***Figure 30***), where no significant difference was found between treadmill and overground walking.

8.3. Segmented Results by Protocol

The last individual segmentation before the final comparison was the influence of the protocol on the collected data. Due to the restricted positioning of the markers in the EDDO protocol, some differences were expected, especially in the rotation plane (third column for all graph sets).

In order to eliminate bias from the other parameters, the following plots compare the trials done with the Helen Hayes protocol while walking overground and captured with the full motion capture system, and the trials done with the EDDO protocol in the same conditions (overground, full motion capture system). Because of this, the noise from the previously discussed EDDO captures is once again visible in the graphs (increase of peaks only in the EDDO mean and standard deviation data).

8.3.1.Results from Test 1 & 2

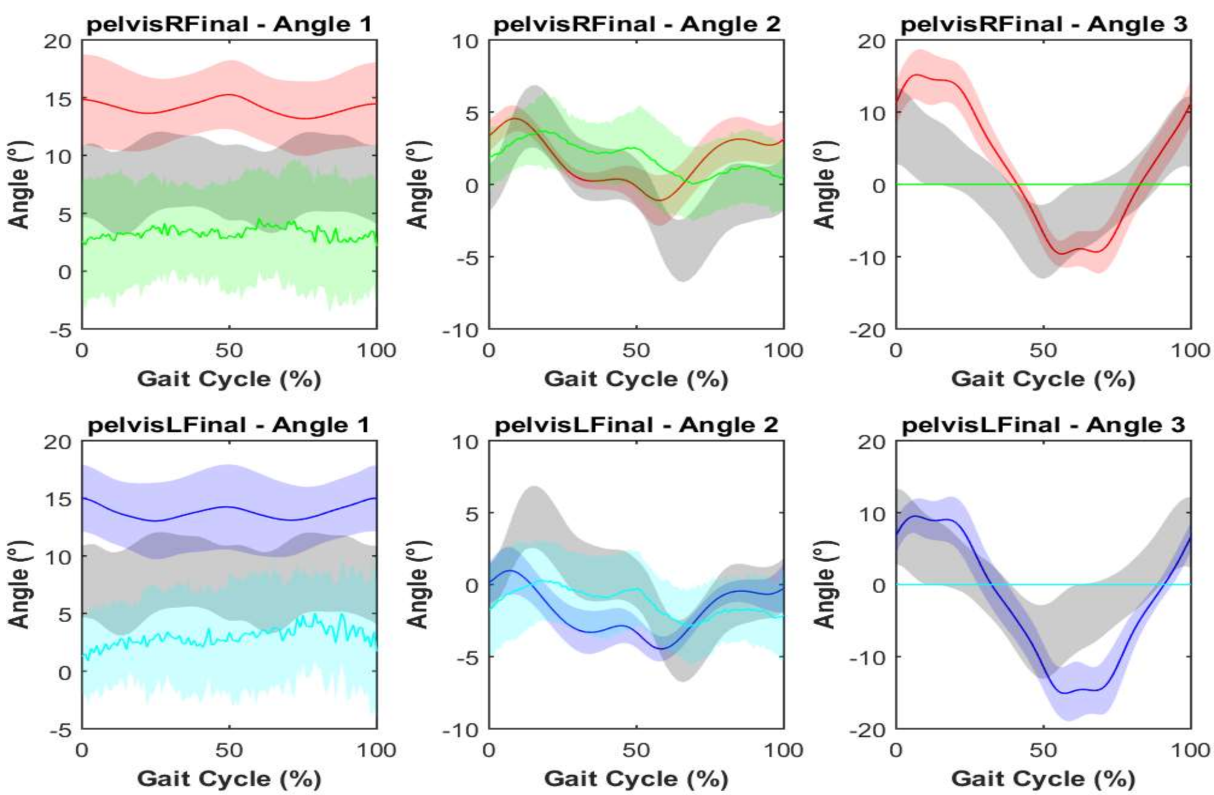

Figure 33. Protocol Comparison for **overground walking trials for the pelvic joint**. Red and blue plots represent the data obtained with the Helen Hayes Protocol, and green and cyan represent the data from the EDDO Protocol.

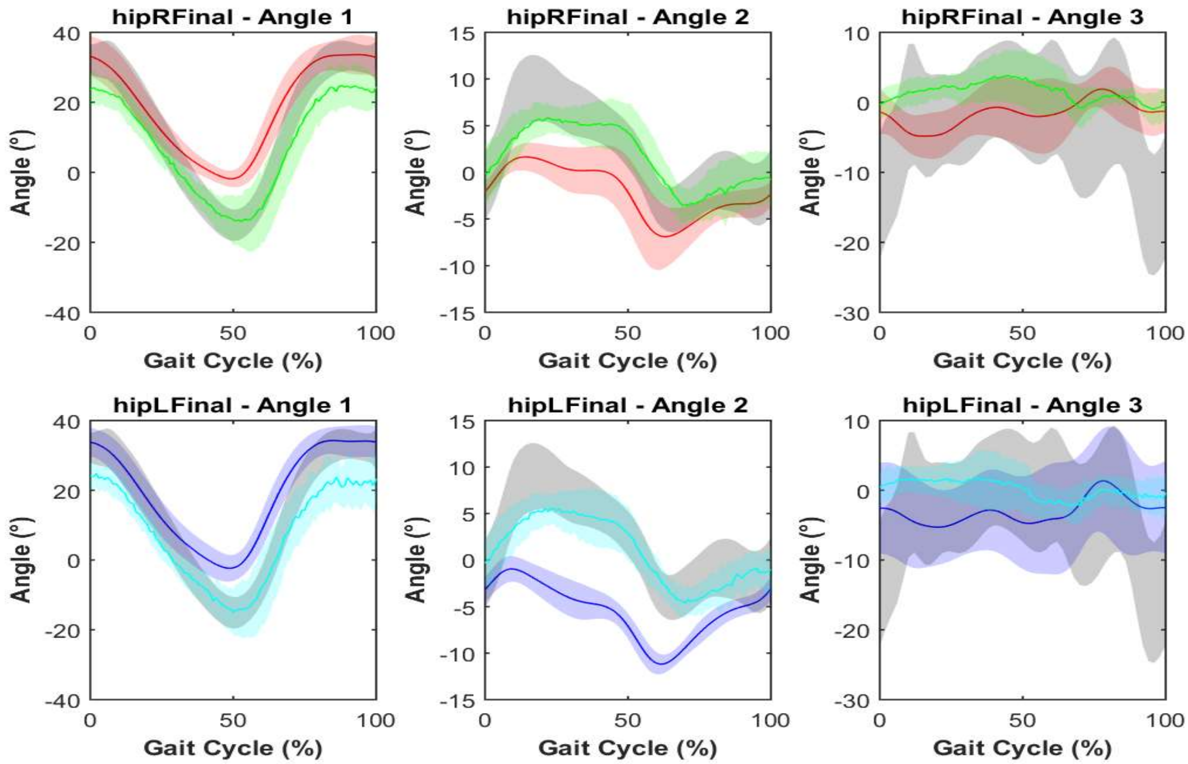

Figure 34. Protocol Comparison for **overground walking trials for the hip joint**. Red and blue plots represent the data obtained with the Helen Hayes Protocol, and green and cyan represent the data from the EDDO Protocol.

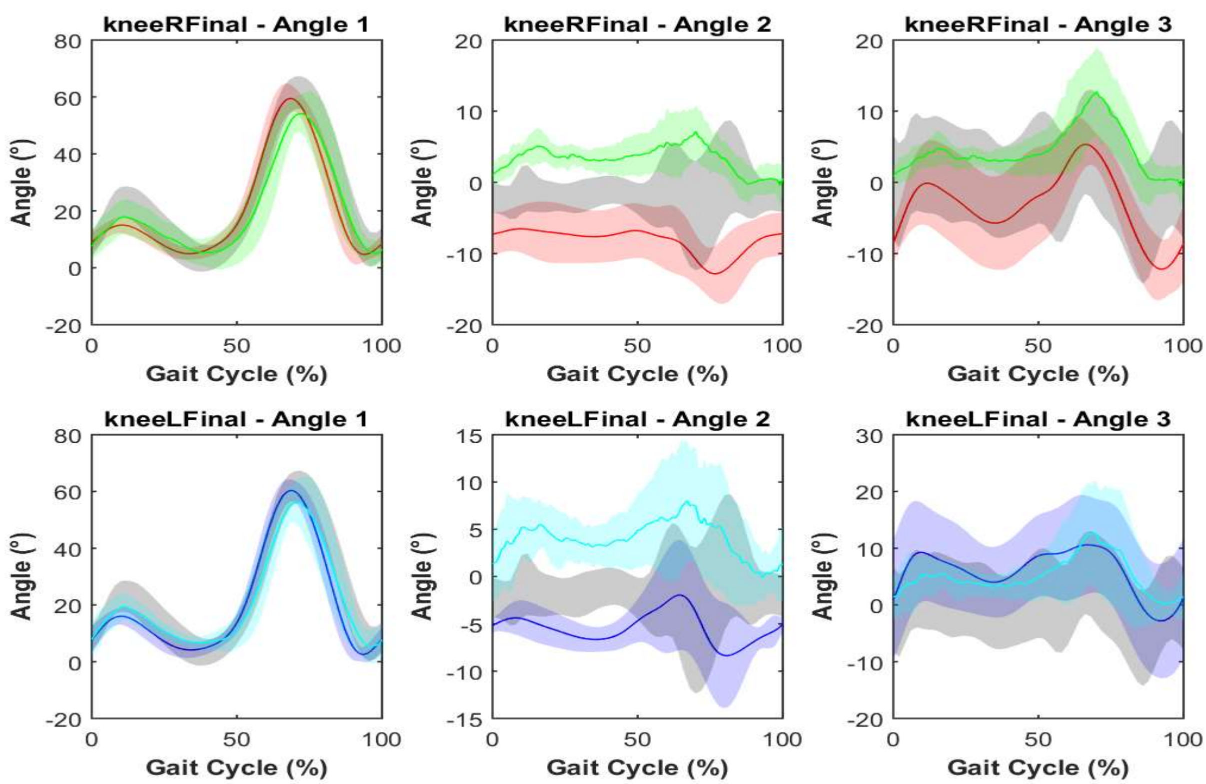

Figure 35. Protocol Comparison for **overground walking trials for the knee joint**. Red and blue plots represent the data obtained with the Helen Hayes Protocol, and green and cyan represent the data from the EDDO Protocol.

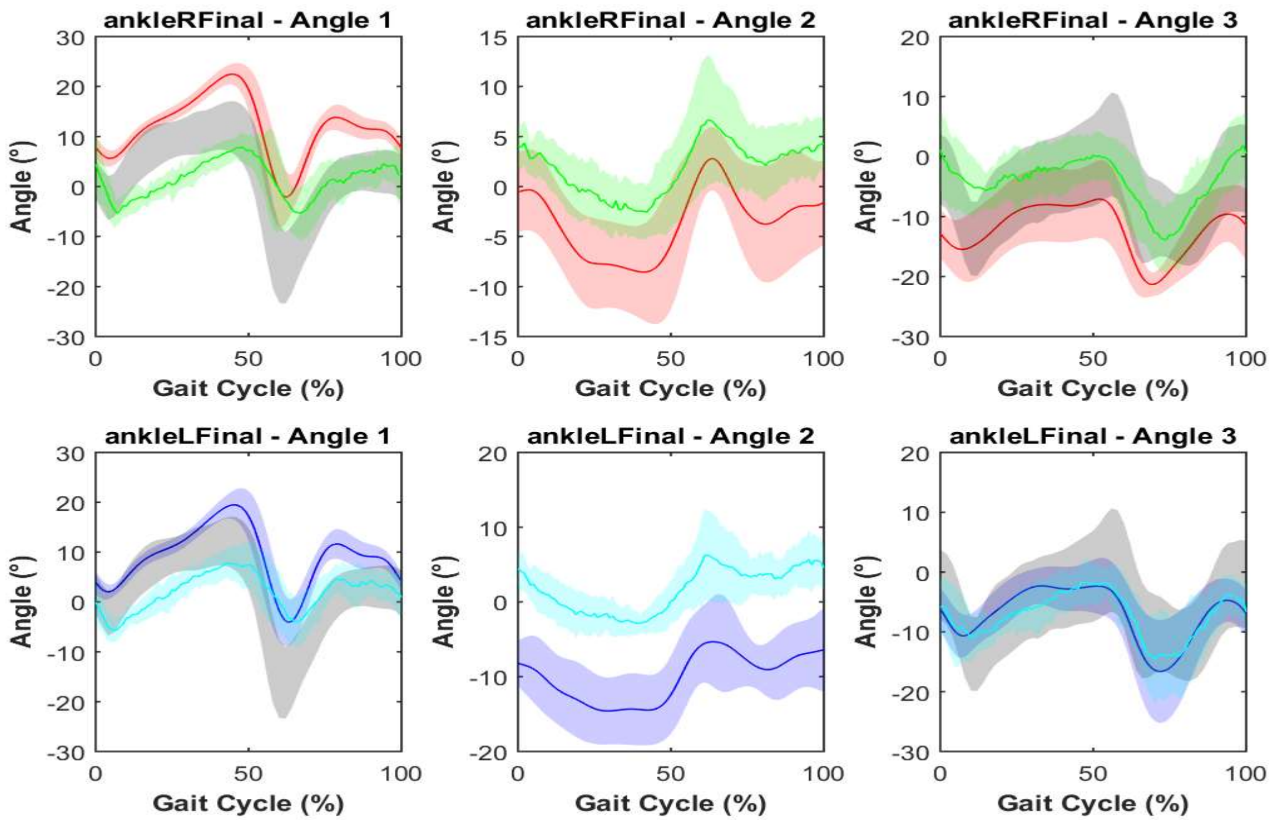

Figure 36. Protocol Comparison for **overground walking trials for the ankle joint.** Red and blue plots represent the data obtained with the Helen Hayes Protocol, and green and cyan represent the data from the EDDO Protocol.

As opposed to the previous comparisons, in this section some more differences are clear. Starting with offsets of 9° increased anterior pelvic tilt, 10° increased hip flexion, 5° increased ankle dorsal flexion, 5° increased knee varus and 5° decreased ankle inversion (on the right) or 10° increased ankle eversion (on the left) for the Helen Hayes protocol. Although some of these offsets are on the margin of the 5° range of clinical comparison, there is a significant offset in the data for pelvic tilt, hip flexion and ankle inversion-eversion as well as a significant difference in knee varus-valgus after toe-off.

At least some of the identified differences are caused by the visibility limitations when using the EDDO protocol, since the restrictive placement of the markers (meant to be seen from only one plane) is feeding the biomechanical model with data that might be missing enough degrees of freedom for a completely accurate 3D reconstruction of the movement.

8.4. Final Comparison of the Protocols

After identifying the sources of the differences between all the setups, the final comparison uses the data from the first test: walking overground with the Helen Hayes protocol using the full motion capture system (considered the gold standard for STT and in the literature), and the data from the third test: walking on a treadmill with the EDDO Protocol using the portable motion capture system (the MoCap method to be validated by STT). The results of the comparison are shown on the following figures.

8.4.1.Results from Test 1 & 3

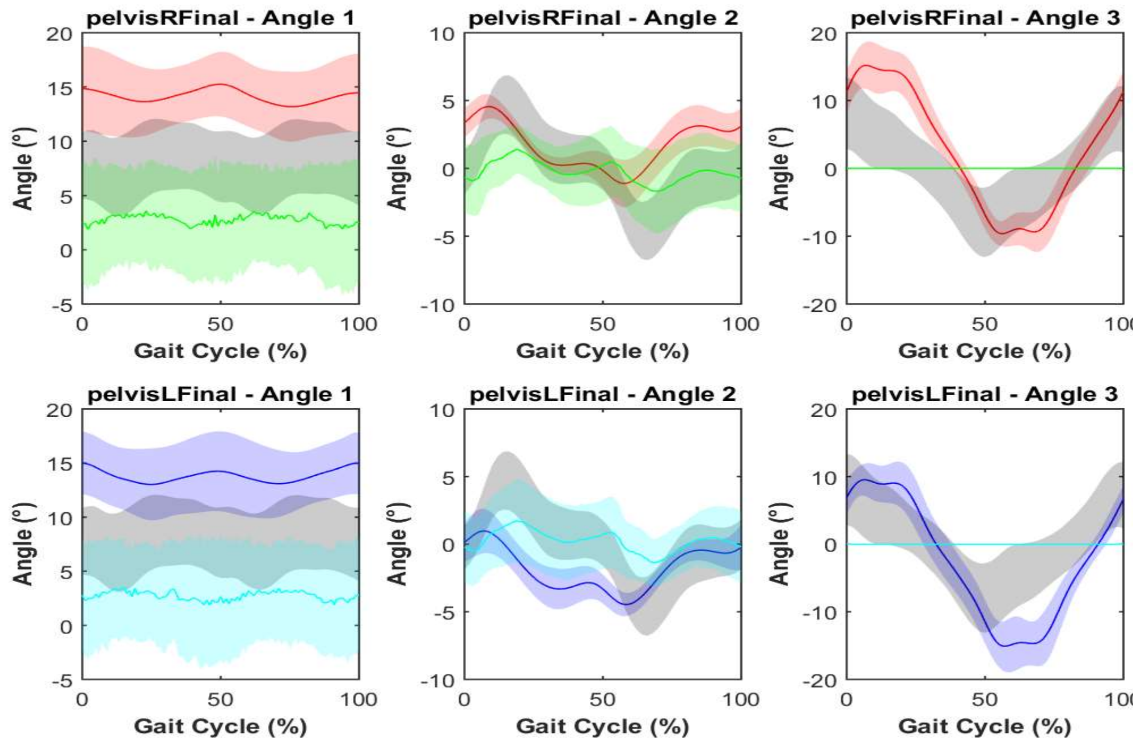

Figure 37. Final Comparison for the pelvic joint. Red and blue plots represent the data obtained with the Helen Hayes Protocol in the preferred setup (overground with the full motion capture system), and green and cyan represent the data from the EDDO Protocol in the preferred setup (on a treadmill with the portable motion capture system).

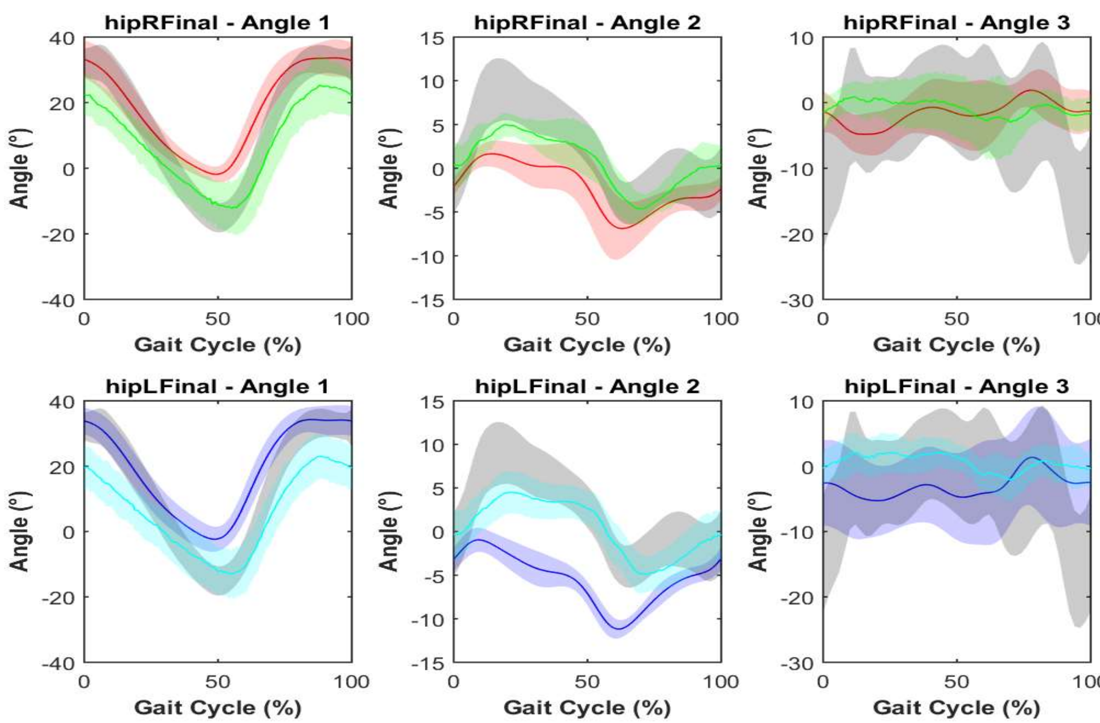

Figure 38. Final Comparison for the hip joint. Red and blue plots represent the data obtained with the Helen Hayes Protocol in the preferred setup (overground with the full motion capture system), and green and cyan represent the data from the EDDO Protocol in the preferred setup (on a treadmill with the portable motion capture system).

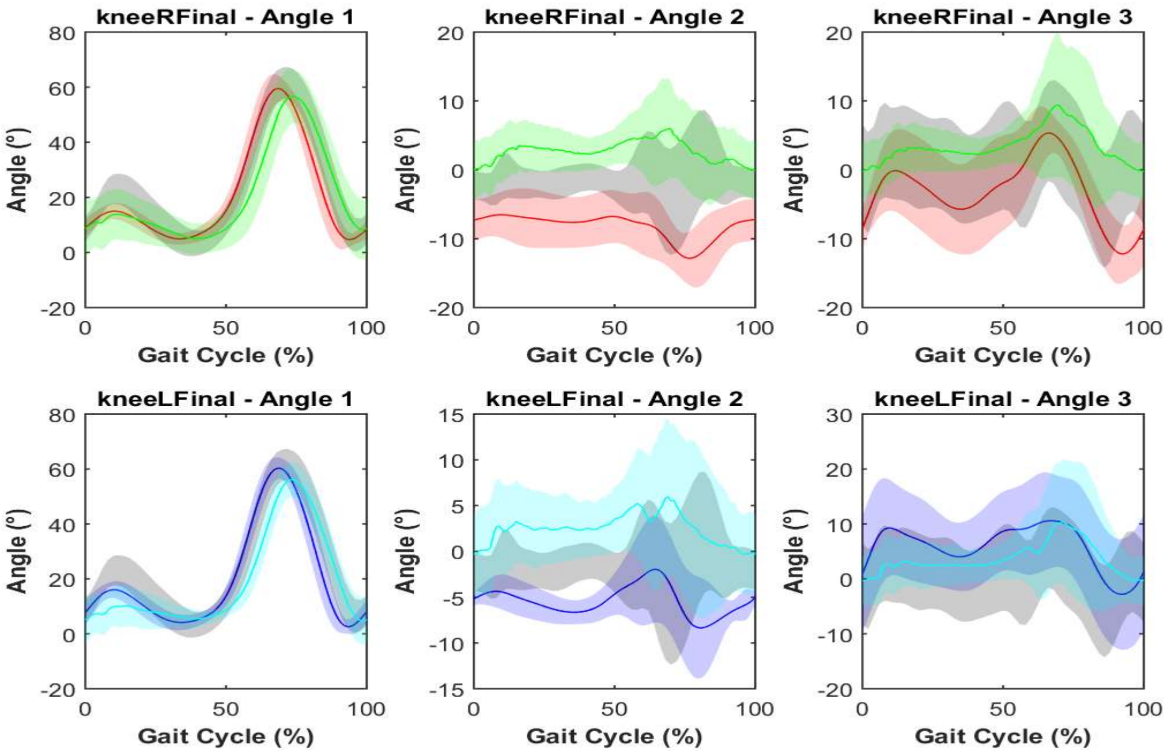

Figure 39. Final Comparison for the knee joint. Red and blue plots represent the data obtained with the Helen Hayes Protocol in the preferred setup (overground with the full motion capture system), and green and cyan represent the data from the EDDO Protocol in the preferred setup (on a treadmill with the portable motion capture system).

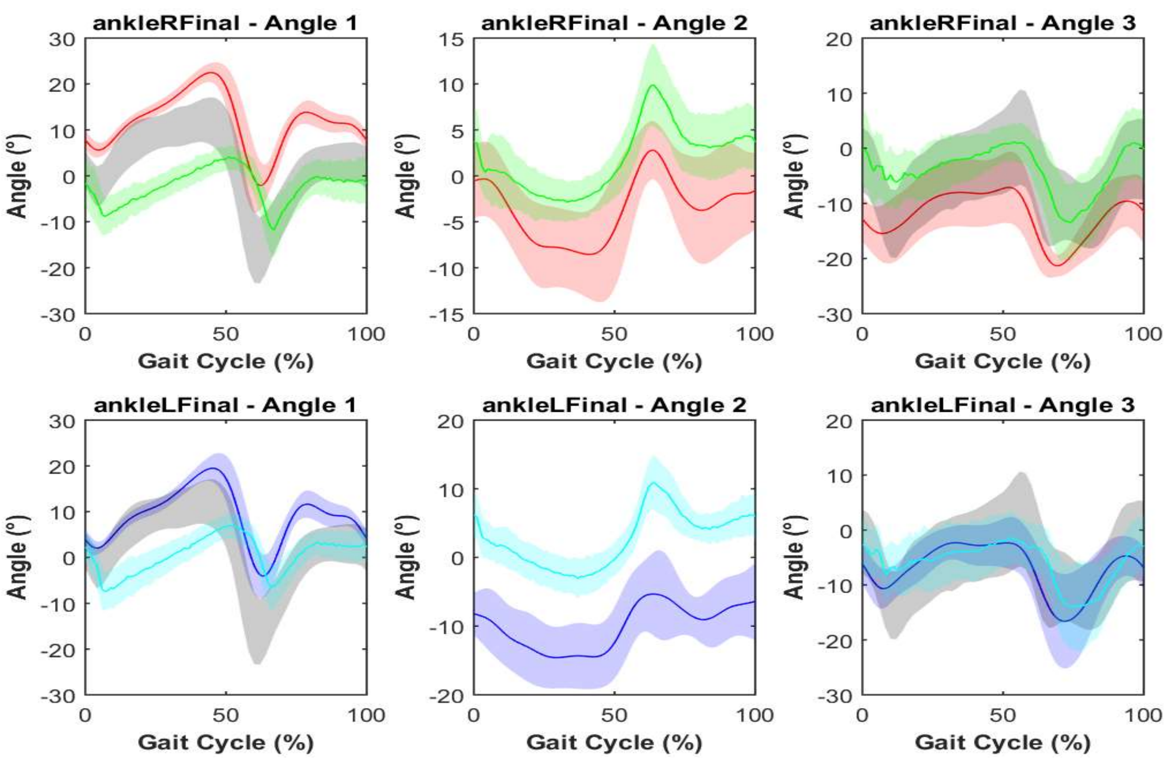

Figure 40. Final Comparison for the ankle joint. Red and blue plots represent the data obtained with the Helen Hayes Protocol in the preferred setup (overground with the full motion capture system), and green and cyan represent the data from the EDDO Protocol in the preferred setup (on a treadmill with the portable motion capture system).

The most notorious differences in this comparison continue to be the ones identified when comparing the protocols, which suggests that the most significant differentiation factor on the validation might be the biomechanical models used to compute the data for each marker set.

It is important that these differences are documented, if not corrected, in order to eventually affirm that the use of the EDDO protocol in its intended setting (on a treadmill with the portable motion capture system) can be equated to the conventional Halen Hayes protocol (overground with the full motion capture system).

Visually, it could be inferred that the offsets that appear on a few of the plots are not a matter of data capture error but a computation mishap due to the comparison of the joint positions during the gait cycle with the calibration data (recorded before each trial). This, and the absence of a wide deviation within trials and subjects, suggests that these offsets might be a systematic error in the data visualization that could be easily corrected, given enough evidence that the error is in fact due to the calibration comparison.

9. CONCLUSIONS

First of all, the successful completion of this project required the participation of several people within STT Systems, since the data and software analyzed especially at the beginning of the timeline depended solely on the documentation of their previous work. Once the necessary datasets and folders were obtained, it was the documentation on it that made the comparison with the literature possible and guided the future documentation that was produced throughout the duration of this project.

One of the main elements to regard about this study is the amount of influencing parameters between the two final datasets to compare. The ideal setup for the Helen Hayes protocol (which is natural overground walking and can only be recorded using the full motion capture system) is a direct opposite of the ideal setup for the EDDO protocol (which involves a treadmill to maintain the same distance between the motion capture device and the subject throughout the trial, and a portable device placed at a specific height lower than the one of the full system). However, many variations of the setups were successfully done and that allowed the data to be compared in several different ways. This resulted in a segmented step-by-step comparison of each influencing parameter that allowed to pinpoint the source of every significant difference in the final protocol comparison.

The step-by-step comparison also allowed for the continuous revision of the setups and the correction of capture errors as the trials were taken. Revisions such as systematic occlusions due to the treadmill location or the angle of the portable motion capture system, capture errors due to the miss-calibration of the floor reference axes or the angle of patient entrance to the motion capture area.

The manipulation of the raw data obtained from the trials was crucial for the final comparison of the results, since a significant amount of different matches needed to be observed and analyzed to reach a conclusion. For this, an organized system was necessary and fundamental, since the amount of data obtained from the experiments was significant.

In accordance to what is shown in the final results, the validation process of the EDDO protocol was successfully completed, and the results suggest the need of an offset revision (or proper documentation) in order to use this protocol as freely as the Helen Hayes protocol is used for clinical gait analysis.

Aside from the slight offsets in a few of the joints and angles, the results shown by the EDDO protocol are satisfactory when compared to the Helen Hayes protocol, because the EDDO protocol allows for the use of a portable device in a less spacious area and it manages to replicate the results of a protocol that requires an entire gait analysis laboratory setup to be recorded.

The main observation regarding data quality for the trials is the varying amounts of noise in the different captures. EDDO plots were, overall, noisier than the Helen Hayes trials. The biomechanical model developed by STT for the Helen Hayes protocol contains a smoothing filter that rids the data of the noise associated with capture precision but the EDDO protocol does not, which explains the striking difference when plotting them in comparison.

Other difference that benefits the Helen Hayes protocol over the EDDO protocol is the marker-set, the EDDO protocol has a more restrictive marker placement, which makes it possible for it to be seen by a portable system. This compromises the data acquisition in some joints and angles due to the visibility restrictions, however, the biomechanical model is robust and it compensates adequately for these cases.

As a last remark, the STT EDDO protocol demonstrates an improvement in the gait analysis acquisition field, by maintaining the most of the accuracy and precision of the trials captured while providing a much more practical hardware solution.

10. PROJECT BUDGET

	Hr. or Units	Price per unit	Total Price
Engineer (Director)	12	75 €	900 €
Engineer (Supervisor)	5	90 €	450 €
Engineer (Student)	300	20 €	6,000 €
Materials (Marker sets, disposable elements)	1	1,000 €	1,000 €
Use of motion capture area and equipment	1	500 €	500 €
Equipment Amortization	1	300 €	300 €
		TOTAL	9,150 €

REFERENCES

Alton, F., Baldey, L., Caplan, S., & Morrissey, M. C. (1998). A kinematic comparison of overground and tradmill walking. *Clinical Biomechanics*, 434-440.

Bell, A. L., Brand, R. A., & Pedersen, D. R. (1989). Prediciton of Hip Joint Centre Location from External Landmarks. *Human Movement Science*, 3-16.

Bovi, G., Rabuffetti, M., Mazzoleni, P., & Ferrarin, M. (2011). A multiple-task gait analysis approach: Kinematic, kinetic and EMG reference data for healthy young adults subject. *Gait & Posture*, 6-13.

Davis, R. B., Ounpuu, S., Tyburski, D., & Gage, J. R. (1991). A gait analysis data collection and reduction technique. *Human Movement Science, 10*, 575-587.

Drawing Academy. (2015). *Drawing Lesson 16, Part 5 – Leg Bones*. Retrieved from Drawing Academy: http://drawingacademy.com/drawing-lessons/leg-bones

Ferrari, A., Benedetti, M. G., Pavan, E., Frigo, C., Bettinelli, D., Rabuffetti, M., . . . Leardini, A. (2008). Quantitative comparison of five current protocols in gait analysis. *Gait & Posture, 28*, 207-216.

Imagine Media. (1995, October). Motion Capture: Optical Systems. *Next Generation Magazine*, p. 53.

Kadaba, M. P., Ramakrishnan, H. K., & Wootten, M. E. (1990). Measurement of Lower Extremity Kinematics During Level Walking. *Journal of Orthopaedic Research, 8*(3), 383-392.

Le Borgne, Y.-A., & Bontempi, G. (2013, 09 24). *Advanced ICT Platform for Rehabilitation.* Retrieved from ICT4Rehab project: http://litpc45.ulb.ac.be/staticICT4Rehab_DMBeta/doc/ICT4Rehab_DM.pdf

McGinley, J. L., Baker, R., Wolfe, R., & Morris, M. E. (2009). The reliability of three-dimensional kinematic gait measurements: A systematic review. *Gait & Posture*, 360-369.

Roetenberg, D., Luinge, H., & Slycke, P. (2013). Xsens MVN: Full 6DOF Human Motion Trackig Using Miniature Inertial Sensors. *XSENS Technologies*, 1-9.

Rozumalski, A., Novacheck, T. F., Griffith, C. J., Walt, K., & Schwartz, M. H. (2015). Treadmill vs. overground running gait during childhood: A qualitative and quantitative analysis. *Gait & Posture*, 613-618.

Schwartz, M. H., Rozumalski, A., & Trost, J. P. (2008). The effect of walking speed on the gait of typically developing children. *Journal and Biomechanics*, 1639-1650.

Sigal, L. (2012, September 21). *School of Computer Science.* Retrieved from Carnegie Mellon University: http://www.cs.cmu.edu/~yaser/Lecture-3-MarkerBasedMocap.pdf

Smith, J. T. (2000). *Methods of Geometry.* NJ: John Wiley & Sons.

Tabakin, D. (2000). *A Comparison of 3D Gait Models Based on the Helen Hayes Hospital Marker Set.* Cape Town: Faculty of Health Sciences at the University of Cape Town.